AD NUMBER

AD826726

NEW LIMITATION CHANGE

TO

Approved for public release, distribution unlimited

FROM

Distribution authorized to U.S. Gov't. agencies and their contractors; Administrative/Operational Use; Jan 1968. Other requests shall be referred to Edgewood Arsenal, Attn: SMUEA-TSTI-T, Edgewood Arsenal, MD. 21010.

AUTHORITY

USAEA Notice, 26 Aug 1971

AD

GCA TECHNICAL REPORT NO. 67-22-G

AEROSOL DISSEMINATION ASSESSMENT

SECOND ANNUAL REPORT

by

A. W. Doyle
P. Lilienfeld
J. F. McCoy
C. Sherman
P. Morgenstern
C. O. Hommel
J. N. Driscoll
A. M. Sacco

January 1968

DEPARTMENT OF THE ARMY
EDGEWOOD ARSENAL
Research Laboratories
Physical Research Laboratory
Edgewood Arsenal, Maryland 21010

Contract DA-18-035-AMC-376(A)

GCA CORPORATION
GCA TECHNOLOGY DIVISION
Bedford, Massachusetts

60

DISCLAIMER NOTICE

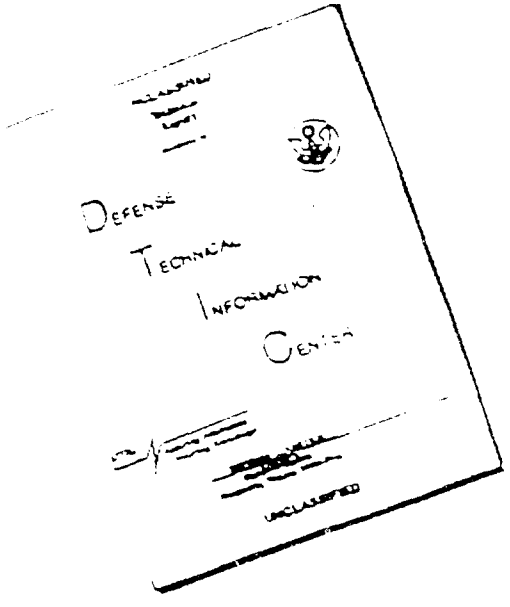

THIS DOCUMENT IS BEST QUALITY AVAILABLE. THE COPY FURNISHED TO DTIC CONTAINED A SIGNIFICANT NUMBER OF PAGES WHICH DO NOT REPRODUCE LEGIBLY.

GCA TECHNICAL REPORT NO. 67-22-G

AEROSOL DISSEMINATION ASSESSMENT

BY

A. W. Doyle
P. Lilienfeld
J. F. McCoy
C. Sherman
P. Morgenstern
C. O. Hommel
J. N. Driscoll
A. M. Sacco

DEPARTMENT OF THE ARMY
EDGEWOOD ARSENAL
Research Laboratories
Physical Research Laboratory
Edgewood Arsenal, Maryland 21010

Contract DA-18-035-AMC-376(A)
Project 1B522301A081

GCA CORPORATION
GCA TECHNOLOGY DIVISION
Bedford, Massachusetts

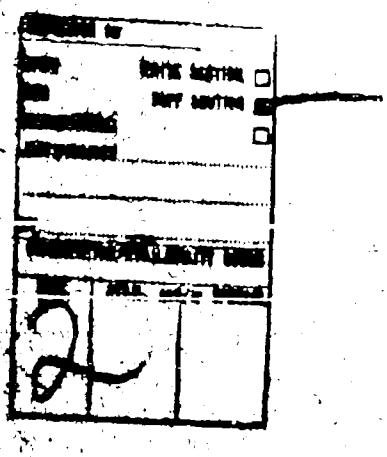

Distribution Statement

This document is subject to special export controls and each transmittal to foreign governments or foreign nationals may be made only with prior approval of the CO, Edgewood Arsenal, ATTN: SMUEA-TSTI-T Edgewood Arsenal, Maryland 21010.

Disclaimer

The findings in this report are not to be construed as an official Department of the Army position, unless so designated by other authorized documents.

Disposition

When this document has served its purpose DESTROY it.

FOREWORD

The work described in this report was authorized under Project 1B522301A081, Chemical Agent Dissemination (U). This work was started in June 1966 and completed in May 1967 for this reporting period.

DIGEST

The program objectives are to develop, to design, and to fabricate a complete system for the assessment of aerosols dispersed in test chambers. The main activities reviewed are aerosol mass decay analysis, chamber mixing and material balance studies, electrostatic effects on chamber aerosols and their evaluation, bioeffectiveness of aerosols, sampling and subsequent data reduction methods required for the determination of aerosol parameters through the mass decay procedure. The design of an automated sequential filter sampling system is described as well as initial phases in the development of a beta absorption-impactor instrument.

Experiments in the above area were conducted both in a large (213 m^3) test chamber with explosive dissemination of agent and simulant materials, and in small laboratory chambers with pneumatic aerosol injection.

TABLE OF CONTENTS

LIST OF FIGURES

LIST OF FIGURES (continued)

LIST OF TABLES

AEROSOL DISSEMINATION ASSESSMENT

I. INTRODUCTION

Basic program objectives which have been outlined in previous reports (Ref. 1-7) are restated here for immediate reference.

The objectives of this program are to develop, design, and fabricate a complete chamber aerosol assessment system. The function of this system is to provide, by the selection and integration of appropriate instruments and analytical methods, a detailed description of chamber aerosols from as near as possible to the instant of dissemination to time periods up to 1 hour. By continuous or incremental sampling, the state of the aerosol should be definable over time intervals as small as 1 second.

Since the system is to be used as a measuring tool in the development of chemical devices, it should be adaptable to the assessment of a broad range of disseminators and agents and to most test chambers now used by groups within Edgewood Arsenal and by contractor organizations. Furthermore, extraneous effects attributable to chamber geometry, aerosol mixing, wall losses, electrostatic charge, and agglomeration should not interfere with proper assessment of disseminator functions.

For a broad capability in aerosol assessment, component instrumentation should permit the following measurements: mass concentration of active agent, concentration of degraded agent and inert materials, descriptive particle-size parameters for active agents, and shape factor for solid particles. In addition to a broad range of particle size, from less than 1μ to 100μ, particle dimensions should be relatable to those describing biological effectiveness of aerosol clouds.

In addition to the requirement that system components should define aerosol cloud properties described above, it is desirable that sensor outputs from these instruments should be amenable to direct display and/or data processing and storage. The extent to which data are displayed or processed and stored for later recall will depend upon which instruments or combinations thereof best meet the system objectives. In certain instances, automation may be highly impractical on the basis of the cost of the process and the accuracy with which measurements can be made with available equipment. Since the aerosol assessment system is to be furnished as a tested, prototype assembly at the end of a 3-year period, the contract framework precludes extensive exploration of new or novel instrumental concepts. Therefore, it has been recommended that commercially available equipment or well-advanced experimental devices be used as the basic system components and that these components be modified and calibrated in accordance with specific system needs.

II. REVIEW OF SECOND YEAR PROGRAM

The techniques and instruments which are to be included in the chamber assessment system were discussed in the Sixth Quarterly Progress Report (Ref. 6). To recapitulate, the basic aerosol measurement concept employs filter sampling with either gravimetric or chemical assessment of the collected mass. Chemical analysis is to be used to discriminate between active agent and background components. Particle sizing is based upon mass decay curve inversion, cascade impaction, light scattering particle counting as a function of time, and microscopic analysis of samples on membrane filters and other plane surfaces. The latter is also employed to distinguish shape factor. Chemical analytical methods are to be implemented by automatic analysis. A variety of other measurements are to be made to support the test analysis including chamber temperature, pressure, humidity, electrostatic effects, etc.

A number of activities have been pursued during the past year to establish the validity of the selected assessment methods and to modify the methods for use in the system.

Mass decay inversion analysis was pursued intensively since this technique has been selected as one of the main tools in the assessment procedures (Ref. 5-7). The design of an automated sequential filter sampler was completed and a sampling system for sequential programmed collection was initiated, and is discussed in the body of this report. The assessment procedure is based upon stirred sedimentation. Therefore theoretical and experimental work was performed to determine the effectiveness of chamber stirring by fans (Ref. 4,5). Analytical studies were performed to permit scaling to large test chambers of the results of mixing experiments performed in the small laboratory chamber (Ref. 7).

Analytical and experimental work was initiated also on the effects of electrical charging of aerosol particles and their behavior in test chambers with electrically conductive and grounded walls (Ref. 7). This study was aimed specifically at assessing the influence of particle charge on the validity of the mass decay analysis for the evaluation of explosively generated aerosols. The initial phases of this work were directed to establish an analytical model for the combined deposition effects produced by space charge induced fields and gravitational settling. Experimental activities were concentrated on space charge measurements by means of a field mill and its correlation with the mass decay of both intentionally charged and uncharged aerosols in a small test chamber.

A review of the present state of knowledge with respect to the deposition properties of aerosols in the respiratory tract was performed and an extensive bibliography on the subject was assembled. This literature analysis pointed out various models which have been suggested for particulate deposition profiles within the human body and the inherent complexity of the biological structure. The pertinence of aerodynamic

size was discussed in terms of the various deposition mechanisms and the direct significance of sedimentation and impaction methods was established (Ref. 7).

The data produced by the assessment system must be usable as input to a material balance. A series of tests was performed in the large aerosol test chamber in which a variety of techniques were evaluated in several attempts to obtain a material balance. A workable method was determined.

Rapid, reliable chemical analytical methods are the cornerstone of the assessment procedures. Several areas related to analysis have been examined. Preliminary work to apply flame photometry as an analytical procedure for the determination of total phosphorus is reported herein. A new method to replace the oxidation step in the current phosphorous procedure was evaluated. The entire filter and deposition material including carbonaceous material is digested in a perchloric acid mixture to assure that all the phosphorus is assayed. This method is also discussed later. Finally, the Technicon AutoAnalyzer system was integrated into the chemical evaluation chain and procedures were developed for the detection of various dissemination materials (Ref. 5).

Laboratory testing of candidate devices led to work in two areas related to aerosol generation. Preliminary experimental work was performed using saccharin and subsequently DOP aerosols. Several generating procedures and apparatus were evaluated to produce aerosols in the size region of interest (a few microns). The condensation generator was rejected because of an insufficient rate of generation. A cascade impactor-spray nozzle combination was tested and found to produce reliable aerosols but its use was discontinued because an excessive fraction of particles was smaller than 1 micron. Finally DOP aerosolization was accomplished using pressurized dissemination with Freon-12. These tests indicate that particle size properties may be controlled by varying the relative amounts of DOP and Freon-12 (Ref. 5).

The problem of unwanted counts registered by the Royco Light Scattering Particle Analyzer with latex calibration spheres was studied. The evidence points to a large spurious population of particles smaller than 0.1 micron which apparently is capable of triggering the circuitry of the instrument. Selective filtration appears to promise a solution to this problem (Ref. 5).

Finally, a new application of beta absorption techniques for mass analysis is being investigated and promises to provide useful backup information for the mass measurements made by filtration techniques.

III. DESCRIPTION OF ACTIVITIES

A. AUTOMATED SEQUENTIAL FILTER SAMPLING

The design was completed and assembly was initiated of an automatic filter sampling system for sequential programmed collection. Manual sampling procedures, although adequate for experimental purposes, are not to be preferred for routine and repetitive measurements. Difficulties are especially apparent during the initial stages of sampling; e.g., shortly after explosive aerosol generation, when a maximum of information has to be gathered in a minimum of time.

The sampling system has been designed to operate as follows:

(1) Preloaded filter holders in a special container will be introduced through an appropriate opening into a sealed "glove box" attached to the side of the assessment chamber. This glove box will contain a multiple filter sampling head, mounted on a base plate riding on slide tracks. The loaded filter holders will be inserted into the sampling head. A door between the glove box and the chamber will be closed during the dissemination event to protect the sampler from shock waves, shrapnel, and other disturbances associated with dissemination.

(2) Prior to dissemination, a manually operated switch will start the sampling pump and apply voltage to electronic circuitry associated with the sampling operation (fan tachometers, flowmeter circuitry, etc.).

(3) About 0.5 minutes after time zero, an operator will open the door separating the glove box from the chamber and slide out the sampling tray with the multiple filter head. This action will trigger the starting of a sequence timer which controls the operation of the solenoid valves. Each filter will operate in sequence and sampling will stop automatically at the completion of the run (about 30 minutes later).

(4) The dissemination event will initiate the operation of a print out timer-flow counter to correlate individual filter sampling with time after aerosol dissemination.

(5) The sampling tray will then be retracted manually into the glove box, the filter holders removed from the sealed environment and placed into a special container and removed from the bottom of the glove box.

The sampling sequence will be programmed by means of plug-ins inserted into the front panel. This feature allows the choice of any number of different sampling sequences such that the 12 filter samples with individual duration of 1/2 minute can be distributed in any way over a total sampling period of up to 50 minutes. In addition the individual sampling period can be extended to 1 minute and the total to 100 minutes.

A rotating cover with automatic indexing will be in front of the filter heads to protect the non-operating filters from direct exposure to the aerosol cloud. During the intermediate dead time (when no filter is sampling) this protective disc will be covering all filters. The indexing mechanism for this cover is programmed by the particular sampling sequence chosen.

Previous experiments have established quantitatively the following sampling parameters:

(1) Total sampling period, after time zero, of approximately 30 minutes.

(2) Sampling intervals of 0.5 minutes.

(3) Minimum desirable number of sampling intervals, approximately 12.

(4) Initiation of first sampling interval, about 1 minute after time zero to allow for adequate chamber mixing.

(5) Initial sampling repetition rate, one every minute, decreasing with time.

(6) Sample flow rate, approximately 1 to 2 cfm for a 1-1/2 inch diameter filter.

Several alternative valving mechanisms for the automated sequential sampling system have been explored. The Gelman sequential sampling head (type No. 1) consists of a circular array of 12 needle values actuated by a "geneva" mechanism. This device was rejected, among other reasons, because it presented an excessive resistance to flow, making it impossible to obtain the desired flow rate. A flow rate of only 0.74 cfm required a pressure drop of 23 inches of Hg across the sequential valve. No other adequate sequential valve mechanism seemed to be available, and thus a system of timer actuated solenoid valves was chosen. Flow measurements were performed on several solenoid valves to establish their flow-pressure drop characteristics, and a valve with a 5/16-inch orifice with a pressure drop of 3.6 inches of Hg at 2 cfm was chosen.

It was decided to measure the total air volume sampled through each filter on an automated basis by means of a turbine flowmeter and to provide electromechanical counter-recorder display of the total flow. Sample concentration will be normalized on the basis of the integrated flow through each filter. Automated constant flow rate by feedback control appears unnecessary and would add unwarranted complexity to the system.

Although only one system of this type is being contemplated at this point, any number of them could be included for simultaneous sampling at various sites within the chamber. The entire sampling system described above is designed for maximum reliability, sturdiness and simplicity of operation, making maximum use of commercially available devices, wherever possible.

B. MATERIAL BALANCE EXPERIMENTS

A series of tests was performed in the large aerosol test chamber in which an attempt was made to recover or account for all of the bomb fill material by sampling the chamber floor, walls and fans as well as the aerosol.

The fill material used for most of these tests was a 1 percent water solution of fluorescent uranine dye. At first the floor was sampled by covering it with trays which were separately washed for recovery of the dye. After the aerosol was sampled, the sum of the floor and aerosol recoveries was less than 100 percent and was variable from test to test. Table 1 summarizes the results of these tests.

Another procedure was tried which avoided the tedious work of washing about 300 trays.

(1) A bomb was fired and the aerosol sampled.

(2) The chamber floor was flooded with several hundred gallons of water. After thorough mixing to dissolve the settled dye the solution was sampled.

(3) A spray was used to wash the fans with an additional measured amount of water which was mixed into the water already on the floor. Another sample was taken.

(4) The overhead rotary nozzle was turned on to wash the ceiling and walls of the chamber into the previous washings and a third sample was taken.

(5) A carefully measured amount of the bomb fill solution was added to the washings which were mixed and sampled again to provide an internal standard for the rest of the analyses.

(6) The aerosol was again sampled.

TABLE 1

FLOOR SAMPLED WITH TRAYS

Test	Device	Fill	Aerosol Recovery Active % Fill	Floor Recovery Active % Fill	Total Recovery Active % Fill	Tray Pattern
447	31	1% U	5.34	72.2	77.54	Strip Across Diameter
448	31	1% U	7.7	76.2	84.5	Strip Across Diameter
449	31	H_2O				
450	31	1% U	6.64	86.9	93.54	Trays Whole Floor
451	31	1% U	5.34	80.7	86.04	Trays Whole Floor
452	31	1% U	16.05	56.4	72.45	Trays Whole Floor
453	31	1% U	8.98	60.4	69.38	Trays Half Floor
454	31	Bis	24	22	46.0	Trays Whole Floor
		Total P	29	28	57.0	

Up to this point the chamber was not vented, and all the dye in the bomb plus the known added amount was assumed to be in the water accumulated on the floor except for a very small amount still suspended in the air.

Table 2 gives the results of three tests using this sequential washing technique. It appeared that for the high mass ratio 31 type bomb substantially all the dye was recovered. With the low mass ratio No. 23 sphere, less than 40 percent of the fill was accounted for. It was concluded that the dye was decomposed or damaged by the dissemination in this bomb.

A 20 percent solution of phosphoric acid in water was disseminated in tests 457 and 459. Samples were analyzed on the Technicon for total phosphorus. Again the total recovery was low. In this case we suspected that the acid reacted with the steel floor of the chamber to form insoluble compounds which adhered to the floor.

Prior to these tests and on another program a few tests were run with Bis and VX filled bombs wherein after the aerosol was sampled and vented from the chamber only the floor was washed with about 10 gallons of isopropanol. The washing solution was sampled and analyzed in the same manner as the filters. Total recoveries were significantly lower than 100 percent, suggesting a significant wall loss. The later tests with uranine solution have indicated that a significant and variable fraction of the fill material ends up on the walls and fans.

The sequential washing of the floor, fans, and walls followed by sampling of the air is necessary for a good material balance. This procedure is workable but presents the following problems.

(1) A dense and lethal aerosol is encountered in carrying out this procedure manually. To avoid this, separate, remotely controlled washing facilities must be provided for floor and fans.

(2) Large amounts of solvent are needed. A minimum of 100 gallons per test is estimated for the large chamber. It is desirable that this solvent be cheap and not form an explosive mixture with the chamber air, and must be compatible with the chemical analysis. The conventional analytical solvent, isopropanol, is unsatisfactory because of expense and for reasons of safety.

Water and aqueous solutions of hexylene glycol and bleach are being considered as inexpensive and safe substitutes for the alcohol. Experiments were conducted to evaluate the solubility of VX in solutions of various strengths and the ability of the analytical methods to recover VX in each of the solutions. The analytical methods of particular interest

TABLE 2

SEPARATE WASHINGS FLOOR – WALLS – FANS

Test	Device % Fill	Aerosol % Fill	Floor % Fill	Fans % Fill	Air Aft. Wash % Fill	Wall % Fill	Total % Fill	Fill
455	31	3.54	95.0	N.S.	.303	N.S.	95.3	U
456	31	5.56	65.5	25.8	N.S.	11.7	103	U
457	23	4.5	15.5	7.5	N.S.	14.4	37.4	Phos.A
458	23	5.1	12.0	7.7	2.6	12.5	34.8	U
459	23	8.3	14.7	2.6	1.8	1.3	20.4	Phos.A

NOTE: U = Ursnine

Phos. A = Phosphoric Acid

N.S. = Not Sampled

were the Schoeniemann method for active agent and the ferric perchlorate hydrogen peroxide method for total phosphorous. Results are shown in Figure 1. VX is stable in a solution of 50 percent glycol even if stored over a weekend, and water alone is an adequate solvent if analyses can be performed immediately.

VX was dissolved in a hypochlorite decontaminating solution and was analyzed by the total phosphorous method. One hundred percent of the VX was recovered, indicating that the "decon" could be used if only phosphorus balance was required.

C. PERCHLORIC ACID OXIDATION OF FILTERS FOR TOTAL PHOSPHORUS

One possible explanation for the difficulty in achieving a material balance in chamber tests is poor extraction efficiencies because of tenacious retention of agent and agent decomposition products on the carbonaceous decay products collected on filters during sampling. Since in the normal analytical procedure only the extract is analyzed, the retained material would not be accounted for. A new method of oxidation was suggested by Mr. A. Koblin of Edgewood Arsenal in which the entire filter is digested in a perchloric acid mixture. The carbon is oxidized, and thus releases the suspected absorbed materials. The laboratory procedure for the method was established for Bis and then at the suggestion of Mr. Koblin for trioctylphosphate (TOP). First determinations were made on solutions of Bis and later with TOP with excellent results in both cases as shown in Figure 2. The materials were then applied to clean filters and carbon coated filters and the ability to recover the material was evaluated. Again, results were excellent with average Bis recoveries of 96 percent in 12 samples with an rms deviation of 1 percent and an average TOP recovery of 97 percent from 7 samples with an rms deviation of 1 percent.

Following the success of this method for Bis and for trioctylphosphate (TOP) its application was attempted on VX. The following kinds of samples were taken:

(1) VX, weighed into a test tube,

(2) VX, weighed onto a filter paper, and

(3) VX, weighed onto a carbon coated filter paper.

In all cases, the sample was covered with the digestion mixture and oxidized. Six aliquots of each were taken, ranging in size from 25λ to 1.00 ml and the color reaction completed. The results were calculated from the best values of the absorbance, that is, when the value was between 0.050 and 0.900. Some of the results are shown in Table 3. There is much too wide a range of recoveries for the method to be useful to us, unless the performance can be improved.

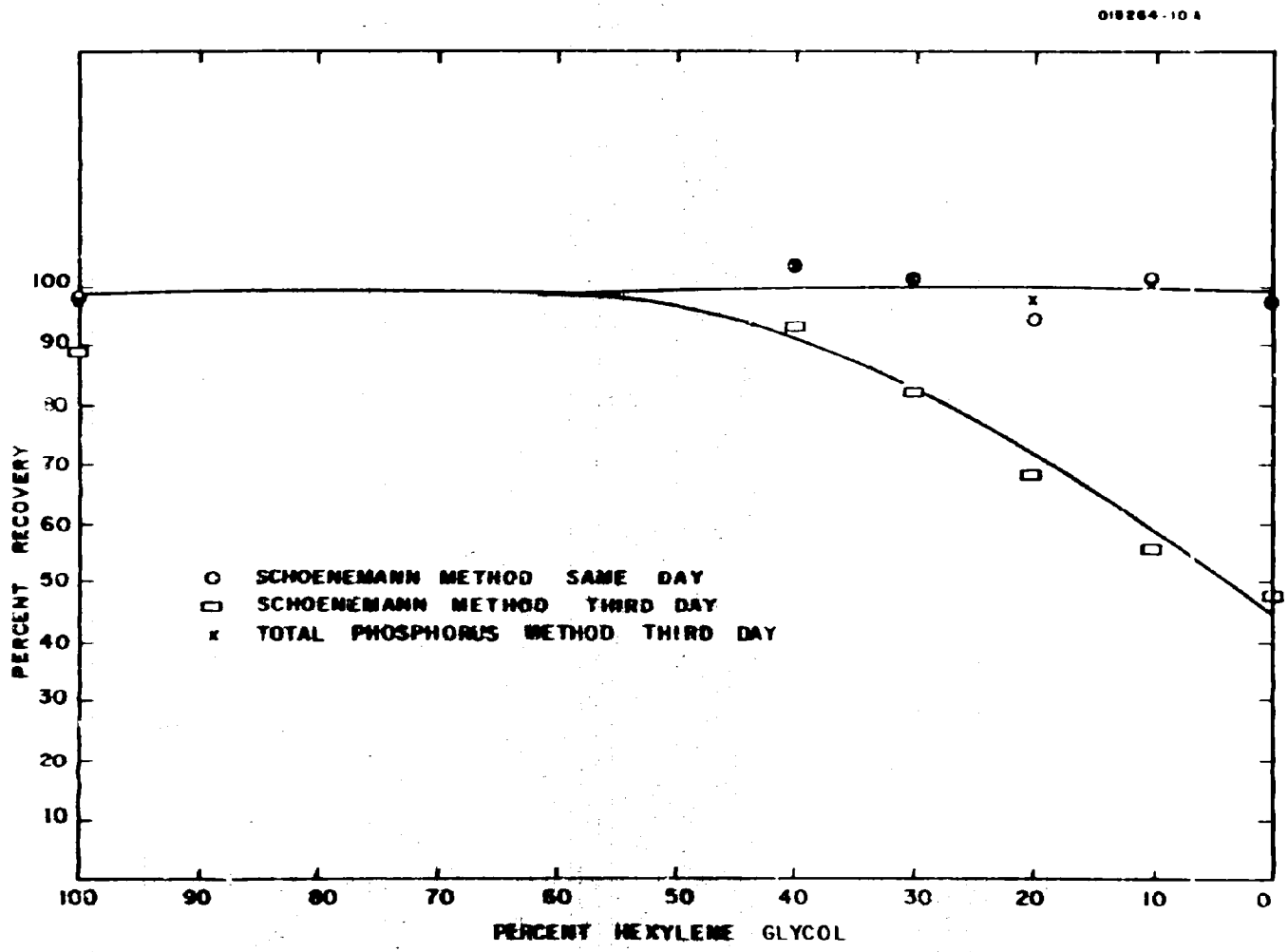

Figure 1. Stability of VX in aqueous solutions of hexylene glycol.

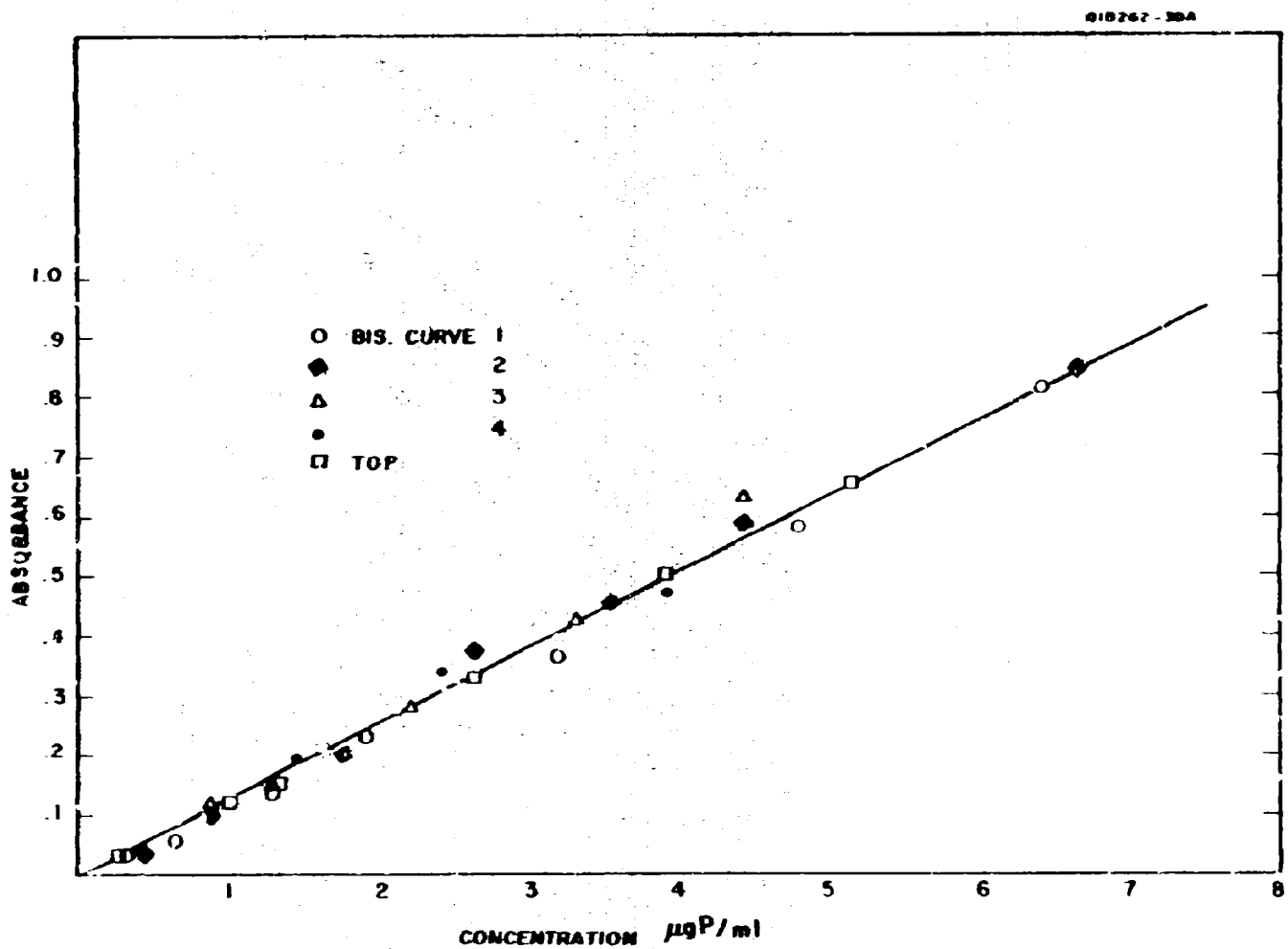

Figure 2. Working curve, BIS and TOP, by perchloric acid method.

TABLE 3

RECOVERY OF VX

Sample	VX Taken mg	VX Found mg	Recovery %
In test tube	11.3	13.3	118
In test tube	23.9	36.9	154
In test tube	49.8	87.5	176
In test tube	9.3	4.7	51
In test tube	48.1	29.1	60
In test tube	8.4	3.5	42
In test tube	21.3	15.9	75
In test tube	47.5	30.4	64
On filter paper	13.5	16.8	124
On filter paper	25.5	44.3	173
On filter paper	45.8	71.8	156
On carbon coated filter paper	10.5	9.7	84
On carbon coated filter paper	24.5	24.2	99
On carbon coated filter paper	50.8	62.7	123

Since the method works so well for Bis and for TOP the difficulty has to be in the oxidation step. Communication with Edgewood Arsenal revealed similar difficultics in applying the perchloric acid oxidation to VX. A literature search of the procedure was made which included a search of the history of the phosphomolybdate color reaction and the materials which interfer. Several possible interferences were uncovered, however, it was concluded that the problem is not one which can be solved simply. The analytical chemistry aspects of this program permit application of methods but do not allow for the development of new analytical methods. It is suggested that the non-reproducibility of the perchloric acid oxidation of VX be investigated in the Edgewood Arsenal laboratories. It is a desirable technique for assessment which we would be pleased to apply if it is worked out in time.

D. AEROSOL MASS EVALUATION BY BETA ABSORPTION

Experiments were reported in the First Annual Report (Ref. 4) on the application of beta absorption measurements for the evaluation of aerosol mass collection on filter substrates. These tests appeared to be discouraging in terms of the sensitivity required for typical sampling volumes.

The technique was subsequently reevaluated in the direction of using a low absorption collection substrate and high collection concentration on a small area.

Initial experimental data were taken to determine the feasibility of using beta radiation absorption through an aerosol deposit collected by impaction on a very thin mylar substrate. The thin mylar base (1/4 mil thick) was used to minimize the absorption due to the substrate and improve the sensitivity of this method. Using a 1 inch diameter C^{14} beta source and collecting treated saccharin aerosol on mylar discs mounted on the impaction plates of a GCA cascade impactor, it was found that this method showed an improvement over the previously reported experiment. The improvement in sensitivity still provided only marginal feasibility, but the results pointed towards modifications in source-detector geometry which would provide the desired sensitivity for the measurement of mass of deposited aerosol. The essential modification appeared to be a significant decrease of the area of the source in order to decrease the amount of particulate deposition to a practical level. A 2 microcurie C^{14} source with an active diameter of less than 1/4 inch was acquired.

It was found necessary to include some collimation of the radiation into the Geiger detector tube to prevent errors due to electron scattering. The collimator consisted of a short cylinder (0.8 cm long) with an inner diameter of about 0.55 cm.

The calibration curve obtained with the above arrangement, using mylar films, is shown on the accompanying graph (Figure 3). The equation of this curve is TR = 100 exp (-0.215S), where Tr is the relative transmission in percent, and S is the area density of the absorber in mg/cm^2. Unattenuated counting rates were about 43,000 counts per minute which for a 1 minute period corresponds to a total error of $2\sqrt{43,000} = 414$ which corresponds to a relative transmission of about 99 percent, thus a 2 percent reduction of transmission appears to be an approximate practical limit of detection. Transmission of 98 percent corresponds to an area density of about 0.1 mg/cm^2 which in turn corresponds to 20 micrograms of materials deposited on a 0.2 cm^2 area (active source area). This sensitivity would be somewhat degraded by the presence of the mylar substrate or collection surface. For a 6.3 micron (1/4 mil) mylar film it is estimated that the limit of detectability would be between 30 and 40 micrograms on a 0.5 cm diameter area. This result seems quite encouraging. The next step should be to collect aerosol on mylar film and corroborate the above conclusions.

The sensitivity obtained with the above geometry corresponds to a minimum of about 1.0 to 1.5 micrograms/liter (flow rate 30 l/m for 1 minute sampling time) compared to the figure of 167 micrograms per liter cited earlier (Ref. 4). Since the estimated minimum desirable sensitivity was about 5 micrograms/liter, this technique seems to offer great promise and will be pursued.

E. ELECTROSTATICS

1. Experimental

The experiments initiated during the seventh quarter on space charge decay measurements in the small test chamber were continued with the main emphasis on correlating these determinations with aerosol mass decay measurements. The prime objective of these tests was to establish the influence of electric particle charges on the depletion rate of a confined aerosol cloud and thus to determine the validity of the mass decay method for the assessment of aerosols. Experience at Edgewood Arsenal and GCA Corporation suggests that anomalous behavior is not encountered when working with explosively disseminated liquids but is much more likely for the case of pneumatically disseminated pre-sized solids. Consequently, the latter was selected for study.

The first set of experiments consisted of the pulsed injection of 0.25 gram samples of saccharin into a small cylindrical test chamber (50 cm diameter x 60.8 cm height, of galvanized steel). The aerosol was injected through a corona charging section (Figure 4). Concurrent measurement of space charge with the field mill, and filter samples for mass decay, were taken over a period of up to 10 minutes after the aerosol injection time.

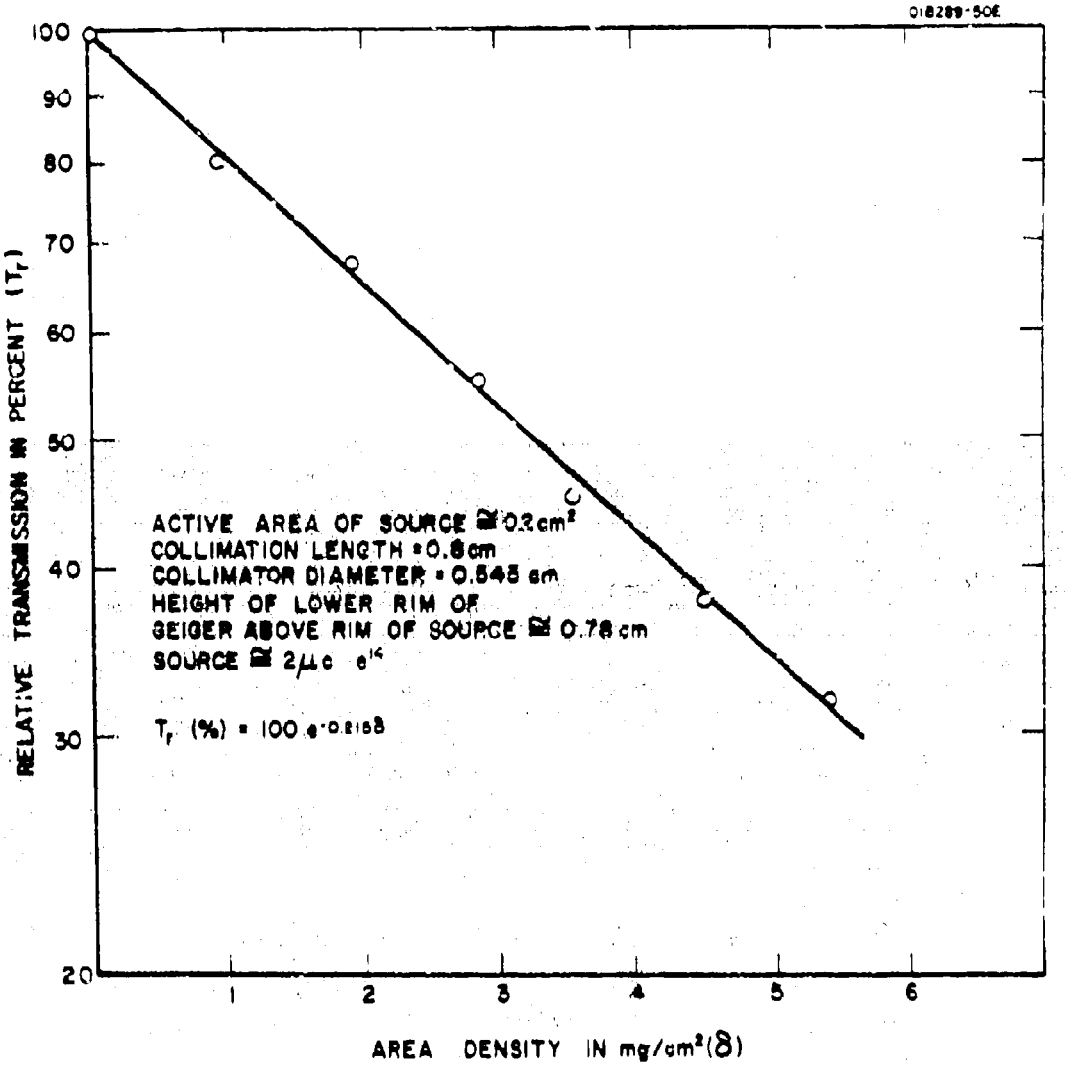

Figure 3. Beta absorption calibration gauge.

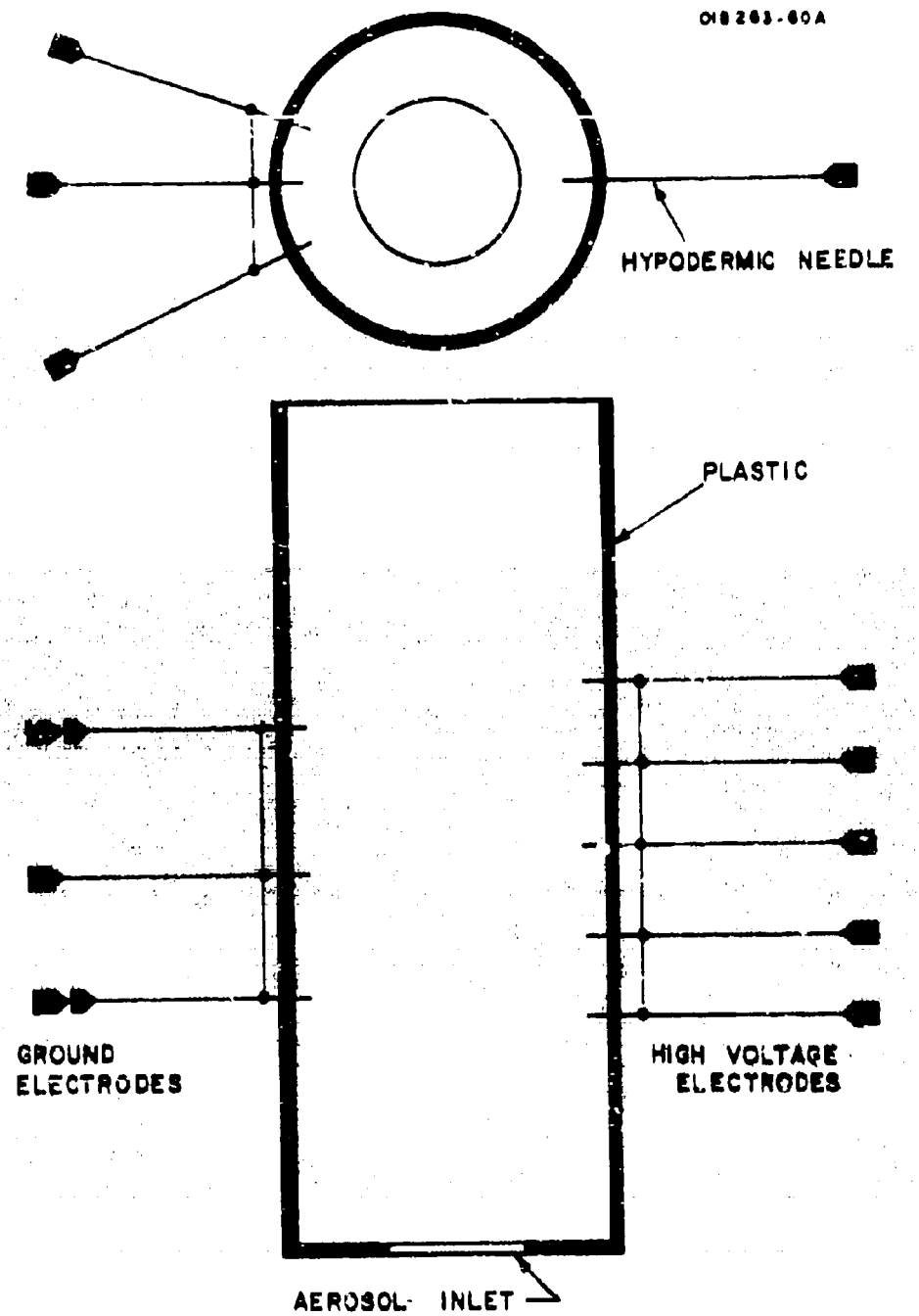

Figure 4. Needle point charger.

The results are shown in Figures 5 and 6. The net space charge measurement was made with a field mill located on the axis and at the top of the chamber. For this geometry, the net space charge density (ρ_o) is given by

$$\rho_o = \frac{2E_z \epsilon_o}{\ell} \quad , \text{(mks)}$$

Where E_z is the field strength measured by the field mill, ℓ is the length of the chamber and ϵ_o is the permittivity of free space. The mass concentrations were determined by filter samples (2.5 liter volume) collected at 1 minute intervals. In figures 5 and 6, the circled numbers are the run numbers and the numbers beside the circles are the voltages applied to the high voltage electrode of the charging section. The sign of ρ_o is the same as the sign of the high voltage electrode.

It can be seen in both Figures 5 and 6 that the data are split into two groups. Since there seemed to be no obvious explanation for this effect, the experiment was rerun to determine if the effect was real or coincidental. The results of this experiment are shown in Figure 7. In this case no significant correlation between mass decay characteristics and charging was observed. Since the above set of results were inconsistant and inconclusive a new improved experiment was performed. The new experiment consisted of the direct measurement of the aerosol lost to the chamber floor and walls and the comparison of the results for cases where there is deliberate charging of the aerosol with cases where there is no deliberate charging. If gravity is the main contributor to the loss process, the bulk of the lost aerosol should be found on the floor. If electrostatics are important in the loss process, this should be reflected in high wall losses.

In order to measure the floor and wall deposition of saccharin, 1/32 inch thick aluminum plates were placed on the floor and attached to the wall of the chamber. The operating geometry of the plates in the chamber is depicted in Figure 8.

It was suggested that the charging section used (Figure 4) might be ambiguous as to where the corona discharge takes place. In order to avoid this difficulty a concentric charger as shown in Figure 9 was constructed. In addition it was found preferable to monitor the charging current instead of the voltage.

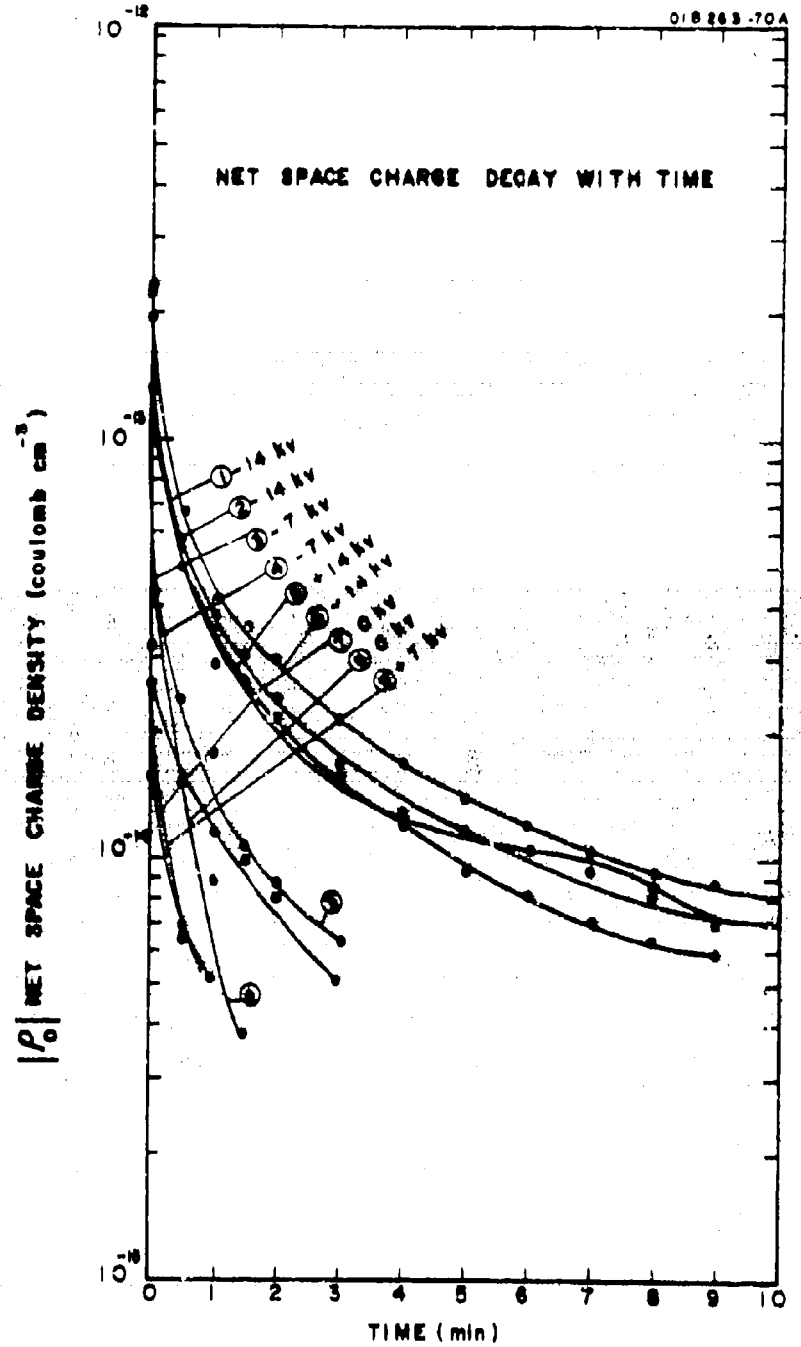

Figure 5. Net space charge decay with time.

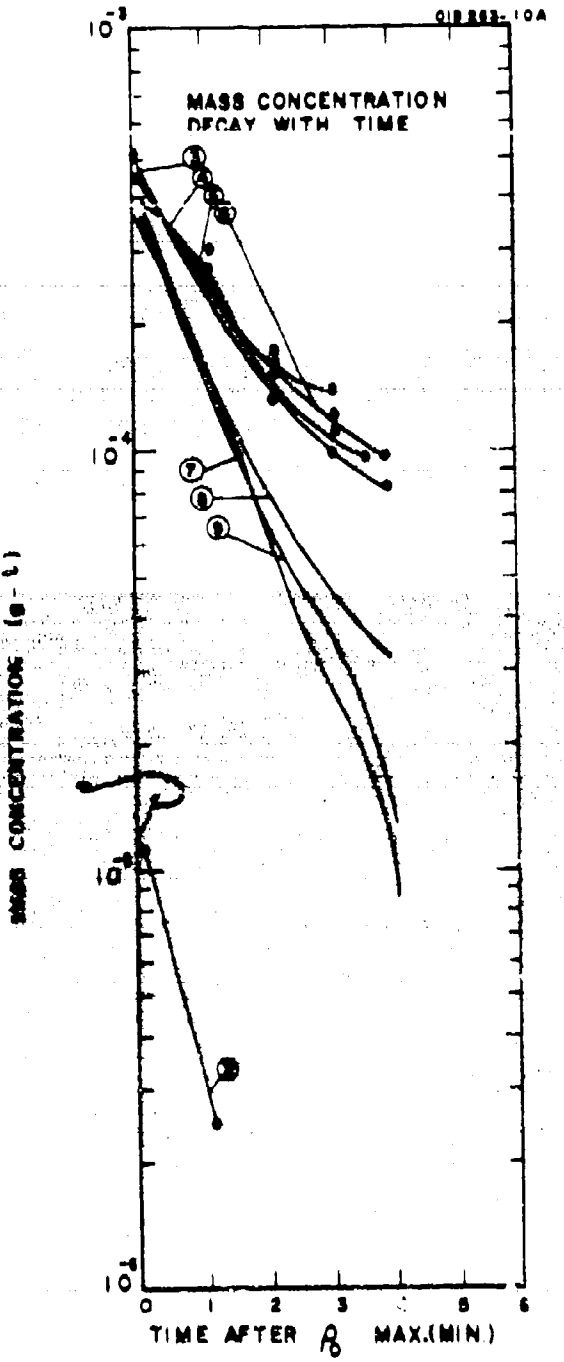

Figure 6. Mass concentration decay with time.

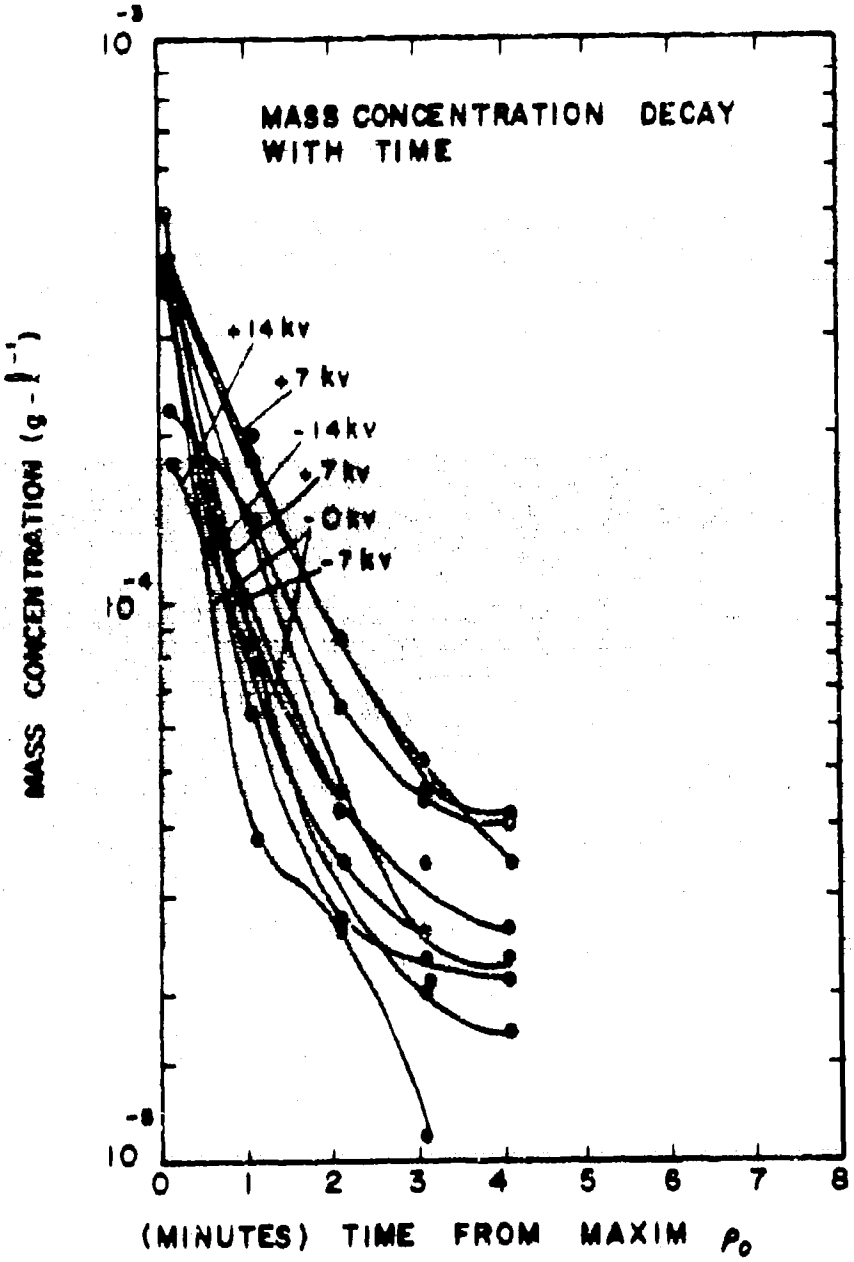

Figure 7. Mass concentration decay with time.

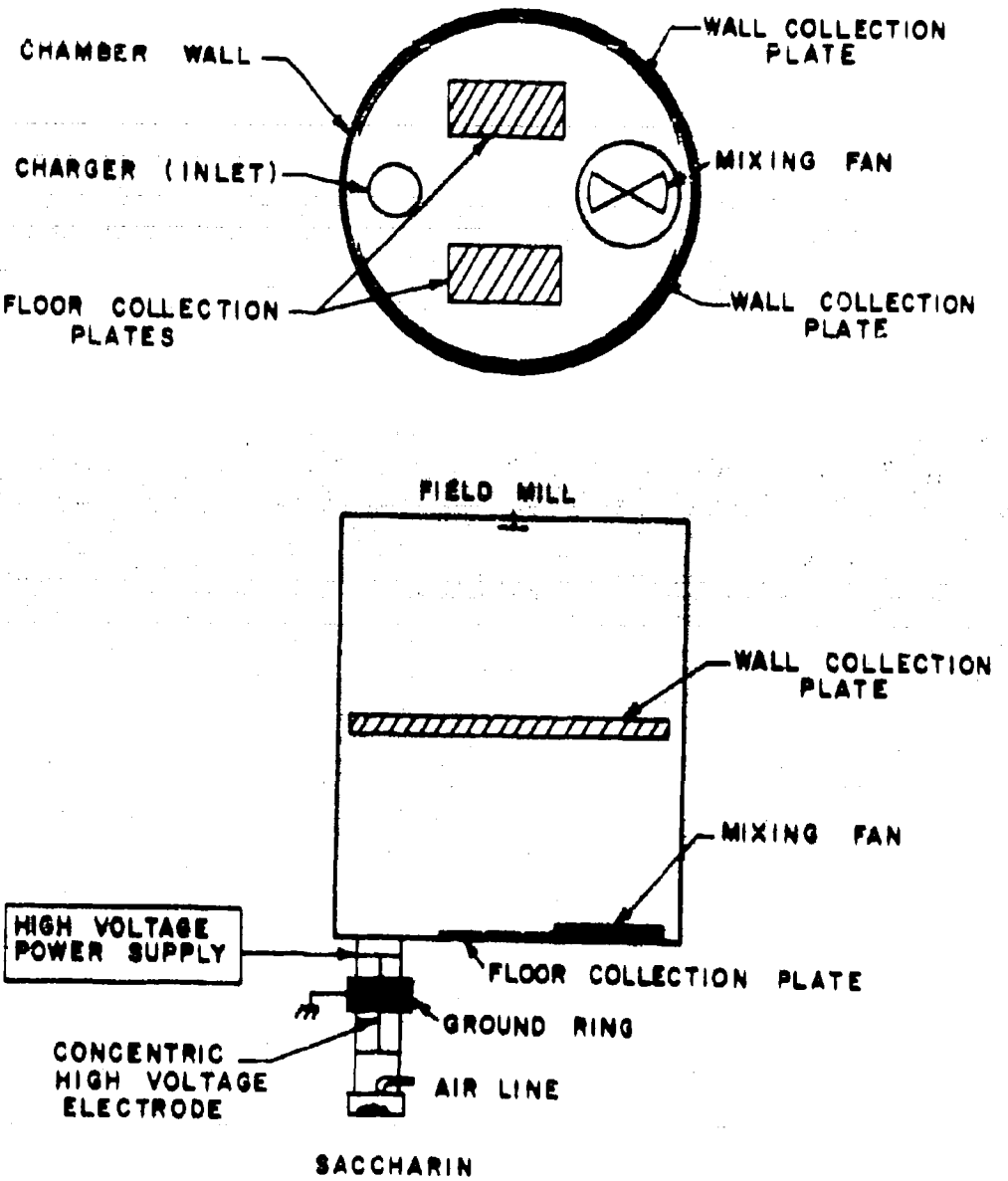

Figure 8. Collection plate geometry.

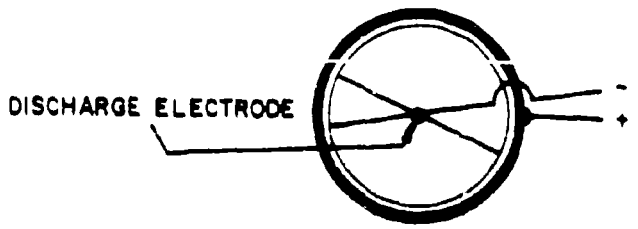

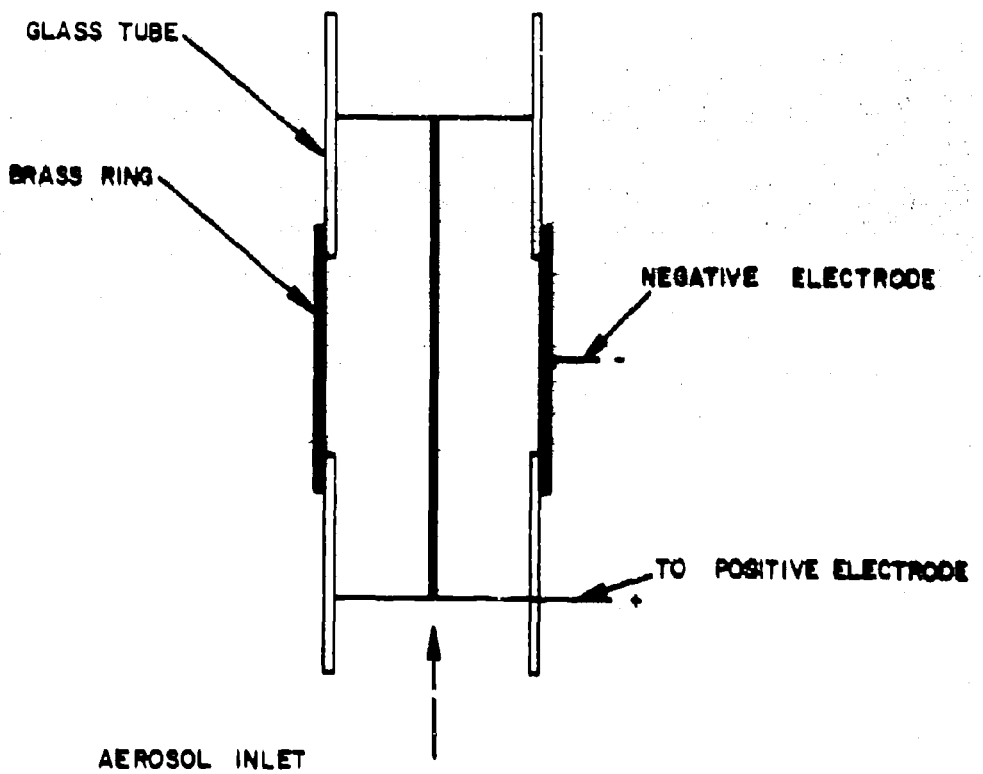

Figure 9. Concentric Charger.

The procedure for these deposition tests was as follows. About 0.25 grams of saccharin were injected into the chamber through the concentric charging section. For five runs the charger was not operated, while for five other runs the center electrode was positively biased such that a corona current of 10 microamps was measured flowing to ground. After injection, the charging section was turned off (for the five runs where applicable) and the saccharin was allowed to settle for 10 minutes with the mixing fan running. At this point, the deposition plates were removed and the mass on the wall plates and the mass on the floor plates were measured. The results of these experiments are shown in Table 4.

Neglecting the eighth run, which shows a somewhat anomalous behavior, the following conclusions are indicated. Wall accumulations are roughly twice as great when the particles are artifically (corona) charged, indicating pronounced electrostatic deposition. Floor mass densities are only slightly affected by artificial charging.

The effect of particle charge on a volume sampling assessment system is given by total mass loss rather than mass density deposition. Thus, averaging the first five and the last four (omitting the eighth run) runs and multiplying by the appropriate floor, ceiling and wall areas, one obtains the results shown in Table 5. The objective of the experiment was to look at the wall and floor depositions and to try to observe a difference between the deliberately charged and the naturally charged cases. Unfortunately the cloud concentration, the amount of material on the fans, and the amount of residue in the disseminator and charging section were not evaluated. This was regretable since the amounts shown in Table 5 do not add up to the 250 mg original sample weight. Tests should be conducted in which all the particles are completely accounted for.

Nonetheless, a very significant difference in deposition pattern was observed for the case of deliberate charging. It is clear that for the case of pneumatically disseminated presized powders the electrostatic forces are playing a definite role in removing particles from the test volume. Further, these results are averaged over the time necessary to remove most of the particles from the volume. At early times, the effects of electrostatic forces would be even more pronounced.

No electrostatic measurements have yet been made in the large test chamber. Since the dimensionless ratio $r_1 q^2 L/\epsilon_0 mg$ is, for constant charge density, five times as large for the large tank as for the small one, the indications are that electrostatic forces will play some role and may even dominate the assessment in the large tank. The significance of this parameter is explained below in the analytic treatment.

TABLE 4

FLOOR AND WALL DEPOSITION, TWO CHARGING CONDITIONS.

No.	Mass Injected	Charger Current	Wall Mass Density	Floor Mass Density
1	0.23g	10 μa	7.1×10^{-3} mg/cm^2	3.1×10^{-2} mg/cm^2
2	0.25g	10 μa	6.6×10^{-3} mg/cm^2	3.5×10^{-2} mg/cm^2
3	0.25g	10 μa	6.4×10^{-3} mg/cm^2	2.9×10^{-2} mg/cm^2
4	0.26g	10 μa	4.5×10^{-3} mg/cm^2	3.5×10^{-2} mg/cm^2
5	0.25g	10 μa	6.6×10^{-3} mg/cm^2	3.3×10^{-2} mg/cm^2
6	0.24g	0	2.0×10^{-3} mg/cm^2	3.1×10^{-2} mg/cm^2
7	0.25g	0	2.0×10^{-3} mg/cm^2	3.1×10^{-2} mg/cm^2
8	0.24g	0	4.8×10^{-3} mg/cm^2	5.1×10^{-2} mg/cm^2
9	0.25g	0	3.2×10^{-3} mg/cm^2	------
10	0.25g	0	3.4×10^{-3} mg/cm^2	3.5×10^{-2} mg/cm^2

TABLE 5

MASS DEPOSITED ON FLOOR AND WALLS FOR TWO CHARGING CONDITIONS.

	Total Mass Deposited on Wall	Total Mass Deposited on Floor
Intentionally (corona) Charged Particles	57 mg	63 mg
"Naturally" (no corona) Charged Particles	26 mg	63 mg

The above considerations do include a number of tenuous assumptions. Thus, it would be necessary to perform electrostatic measurements in the large chamber to test these considerations directly. A conclusion drawn from these tests is that for the case of pneumatically disseminated dry powders a serious error could be introduced if only gravitational settling is assumed for mass concentration decay without a correction procedure for loss due to electrostatic effects on the wall, ceiling, and floor of the chamber.

Future work in this area is expected to clarify this problem, and tests along these lines are being planned for the large (213 m^3) chamber.

2. Analytical

A theoretical treatment of the settling of particles by combined gravitational-electrostatic has been made.

a. Monopolar Charging

The problem being considered here is the following.

For the case where an aerosol cloud of particulate matter is introduced into a container having an electrically conducting inner surface, it is desired to obtain the law by which particles are removed from the volume and deposited on the surface. It will be assumed that the interior of the container is divided into two regions:

(1) A thin boundary layer in which the gas in the container is assumed to be motionless.

(2) A region outside the boundary layer in which the gas is stirred in such a way as to create a homogeneous distribution of particulate matter.

It may be remarked at this point that this division may, as far as practice is concerned, be open to some question. Beside questions concerning the realizability of homogeneity in the interior region, there is also a problem concerning the relative thickness of the boundary layer and a "persistance length" of a particle once set into motion. In order that this division be valid, the boundary layer must be many times the distance over which particles are brought to a constant velocity. For present purposes, these questions will not be examined further, and this division will be made.

Consider first the arrangement shown in Figure 10, a cylindrical container and particles of a single size and charge. The more complicated cases of particles charged both positively and negatively and of varying magnitude of charge and diameter will be deferred to a later report. The following notation supplements the notation given in Figure 10:

R	-	Cylinder radius
L	-	Cylinder height
A_1	-	Cylinder end area
A_2	-	Cylinder side area
N	-	Total instantaneous number of undeposited, charged particles in container
n	-	instantaneous number density of undeposited charged particles in container

n_1 - initial number density of charged particles
q - charge per particle (assumed constant)
a - particle diameter
m - particle mass
g - gravitational acceleration
η - coefficient of viscosity
v_g - drift velocity due to gravity
v_f - drift velocity due to electric field
E - average value of electric field at the container wall
ϵ_0 - permittivity of free space ($10^{-9}/36\pi$)

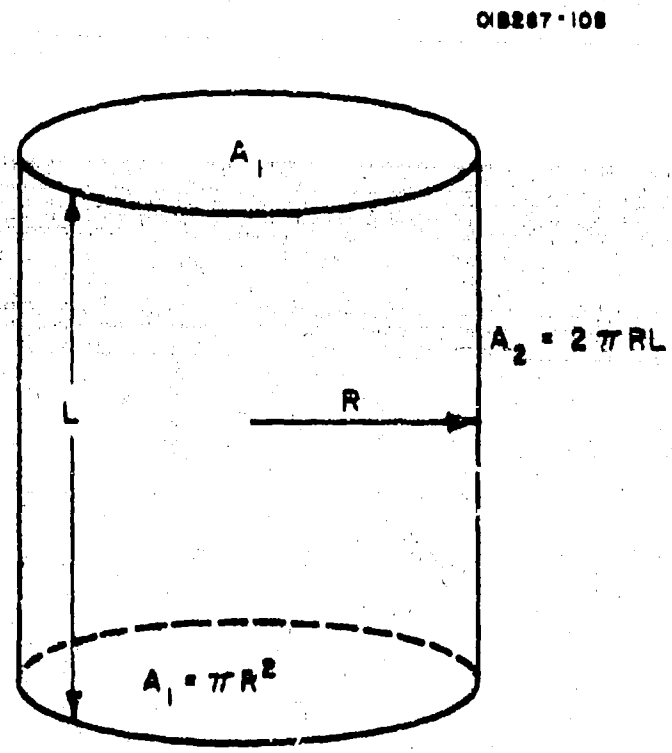

Figure 10. Definition of symbols.

Since the particles are considered to be charged, in addition to a downward gravitational drift over the lower area A_1, the particles are acted on by an electric field, the source of which is the net charge on the particles themselves.

The balance equation for deposition will be

$$\frac{dN}{dt} = A_1 L \frac{dn}{dt} = - A_1 n v_g - (2A_1 + A_2) n v_f \qquad (1)$$

The drift velocities are obtained by assuming that Stoke's law holds in the boundary layer,

$$6\pi n a v_g = mg \qquad (2)$$

$$6\pi n a v_f = qE \qquad (3)$$

E, the value of the electric field at the surface of the container will for a cylinder, vary over the surface. For our purposes, however, a representative value of E may be obtained by an elementary application of Gauss' law.

$$qn \pi R^2 L = (2\pi R^2 + 2\pi RL) E \epsilon_0 \qquad (4)$$

Putting Equations (2), (3) and (4) into Equation (1), and replacing A_1, A_2 by their equivalents in R, L, one obtains

$$\frac{dn}{dt} = - \left(\frac{mg}{6\pi n aL}\right) n - \frac{q^2}{6\pi n a \epsilon_0} n^2 \qquad (5)$$

The solution of Equation (5) subject to the initial conditions

$$n = n_1$$

$$t = 0$$

is

$$n = \frac{n_1}{\left(\frac{n_1 q^2 L}{mg \epsilon_0} + 1\right) \exp\left(\frac{mg}{6\pi n aL} t\right) - \frac{n_1 q^2 L}{\epsilon_0 mg}} \qquad (6)$$

For $q = 0$ one obtains

$$n = n_1 \exp\left(-\frac{mg}{6\pi \eta a L}\, t\right) \tag{7}$$

the usual gravitational settling law.

For

$$\frac{n_1 q^2 L}{mg \epsilon_o} \gg 1 \gg \frac{mg}{6\pi \eta a L}\, t \tag{8}$$

one obtains

$$n = \frac{n_1}{1 + \frac{n_1 q^2}{6\pi \eta a \epsilon_o}\, t} \tag{9}$$

the common expression associated with square law recombination. The relative influence of electric field and gravity at early times is thus obtained from the dimensionless ratio $n_1 q^2 L/mg\epsilon_o$ as can be seen directly by inspection of Equation (5).

Equation (6) applies only to those particles which contribute to the net charge in the tank. Uncharged particles are removed only by gravitational settling and hence always settle according to a law of the type given by Equation (7). If the initial particle density for neutral particles is n_2, then the total number densities at time t will be given by

$$n = \frac{n_1}{\left(\frac{n_1 q^2 L}{mg \epsilon_o} + 1\right) \exp\left(\frac{mg}{6\pi \eta a L}\, t\right) - \frac{n_1 q^2 L}{\epsilon_o mg}} + n_2 \exp\left(-\frac{mg}{6\pi \eta a L}\, t\right)$$

b. Numerical Example

Having derived equations for the settling rate of particles under combined gravitational-electrostatic forces, these equations will now be applied to the settling occuring in two of the experimental systems used at GCA, a small cylindrical metal tank and a much larger cylindrical tank, also with an electrically conducting

interior. The examples treated are for an aerosol consisting of saccharin particles, assumed to have a single size and mass. The pertinent numbers are:

Small tank - diameter 50 cms; height 60 cms

Large tank - diameter 6.1 meters; height 7.3 meters

Particle diameter - 5 microns

Particle density - 1 g/cm^3

Total mass injected into small tank 0.25g

Total mass injected into large tank 200g

Acceleration of gravity $\simeq 10^3$ cgs = 10 mks

Single (spherical) particle mass : 6.25×10^{-11} g

Coefficient of viscosity of air : 1.8×10^{-4} cgs

(1) Exponential Time Constants

$$\tau = \frac{6\pi \eta a L}{mg} = \frac{6\pi \times 1.8 \times 10^{-4} \times 5 \times 10^{-4} \times 1}{6.25 \times 10^{-11} \times 10^3}$$

= 27 minutes (small tank)

= 6 hours (large tank)

(2) Dimensionless Ratio $n_1 q^2 L/\epsilon_0 mg$

This ratio involves electrostatic quantities and mks units will be used when convenient.

$$\text{Total particle density} = \frac{\text{Total particles}}{\text{volume}} = \frac{\text{Total mass}}{\text{mass/particle} \times \text{volume}}$$

$= 3.42 \times 10^{10}/m^3$ for the small tank

$= 1.5 \times 10^{10}/m^3$ for the large tank

If it is assumed that $n_1/n_1+n_2 = 1/5$, then

$n_1 = 6.84 \times 10^9/m^3$ for the small tank

$n_1 = 3.0 \times 10^9/m^3$ for the large tank

The average charge per particle, q, may be found approximately by a crude application of Gauss' law. Thus, if it is assumed that the field is constant over the whole interior surface of the tank, Gauss' law gives

$$q = q = \frac{2\,(K+L)\,E\,\epsilon_o}{n_1\,RL}$$

Typical values for E, found by use of a field mill in the small tank, are of the order of 10^4 volts/meter, when injected particles are charged by corona and of the order of 1/10 this value when naturally charged. Using the higher (corona charged) value, one obtains $q = 1.45 \times 10^{-16}$ coulomb for the small tank and the large tank (since the charge depends on the charging process and not the tank). Using all of these values one obtains

$$\frac{n_1\,q^2L}{\epsilon_o\,mg} = 15.6 \quad \text{for the small tank}$$

$$= 83 \quad \text{for the large tank}$$

Thus, for these conditions a fraction n_1/n_1+n_2 of the total injected particles is initially more influenced by electrostatic than by gravitational forces. Ultimately of course, with passage of time, Equation (6) reverts to an exponential law once again, but for such times $n/n_1 \ll 1$ and assessment measurements may be difficult to make.

c. Bipolar Charging

In this section the problem is extended to include charges of both signs. The time histories of the charged particles are described by two coupled, nonlinear, simultaneous differential equations for the particles having plus and minus charge. A single integral is obtained, and this leads to a decoupling of the equations: the resulting equations containing only a single dependent variable are still nonlinear, and cannot be solved in terms of elementary functions. Further effort is required to either solve these equations numerically, find approximate methods of solution, or solve simpler equations which may be used to place upper and lower bounds on settling rates. The following parameters are added to the prior notation list.

n_o - number of density of neutral particles
n_+ - number of density of positively charged particles
n_- - number of density of negatively charged particles

For further details of the problem being treated, refer to the treatment of monopolar charging.

The equations for deposition for the three types of particles are

$$A_1 L \frac{dn_o}{dt} = - A_1 n_o v_g \qquad (10)$$

$$A_1 L \frac{dn_+}{dt} = - A_1 n_+ v_g - (2A_1 + A_2) n_+ v_g \qquad (11)$$

$$A_1 L \frac{dn_-}{dt} = \begin{cases} 0 & \text{if } v_f > v_g \\ -A_1 n_- (v_g - v_f) & \text{if } v_f < v_g \end{cases} \qquad (12)$$

For the case $v_f > v_g$, the solution of Equation (12) is $n_- =$ constant, and the solution for n_+ reverts back to one similar to that found for the case of settling in the presence of particles of one sign.

In general, setting $A_1 = \pi R^2$, $A_2 = 2\pi RL$, using Stokes's law,

$$6\pi a v_g = mg$$

$$6\pi a v_f = qE$$

and Gauss law

$$q(n_+ - n_-) \pi R^2 L = (2\pi R^2 + 2\pi RL) E \epsilon_o$$

one obtains

$$L \frac{dn_o}{dt} = - n_o \frac{mg}{6\pi a} \qquad (10a)$$

$$L \frac{dn_+}{dt} = - n_+ \frac{mg}{6\pi a} - n_+ \left[\frac{q^2 (n_+ - n_-) L}{\epsilon_o 6\pi a} \right] \qquad (11a)$$

$$L \frac{dn_-}{dt} = \begin{cases} 0 & \text{for } v_f < v_g \\ - n_- \left[\frac{mg}{6\pi a} \right] - n_- \left[\frac{q^2 (n_+ - n_-) RL}{2 \epsilon_o (R+L) 6\pi a} \right] & \text{for } v_f > v_g \end{cases} \qquad (12a)$$

Let $\tau = \frac{mg}{6\pi a L} t$

and

$$n_o(0) = n_1$$

$$n_+(0) = n_2$$

$$n_-(0) = n_3$$

$$n_i = n_1 + n_2 + n_3$$

$$X = n_o/n_i$$

$$Y = n_+/n_i$$

$$Z = n_-/n_i$$

$$X_o = n_2/n_i$$

$$Y_o = n_2/n_i$$

$$Z_o = n_3/n_i$$

$$\frac{n_i\, q^2 L}{\epsilon_o\, mg} = \alpha$$

$$\frac{n_i\, q^2 L\, R}{2\, \epsilon_o\, mg\, (R+L)} = \beta$$

Then

$$\frac{DX}{d\tau} = -X \qquad (10b)$$

$$\frac{DY}{d\tau} = -Y - \alpha Y\,(Y-Z) \qquad (11b)$$

$$\frac{DZ}{d\tau} = \begin{cases} 0 & \beta\,(Y-Z) \geq 1 \\ -Z + \beta Z\,(Y-Z) & \beta\,(Y-Z) \leq 1 \end{cases} \qquad (12b)$$

The equations are now in fully non-dimensionalized form, and the initial conditions are $X = X_o$, $Y = Y_o$, $Z = Z_o$, $\tau = 0$.

Multiply Equation (11b) by β/Y, Equation (12b) by α/Z and add

$$\frac{\beta}{Y}\frac{dY}{d\tau} + \frac{\alpha}{Z}\frac{dZ}{d\tau} = -2 \qquad (13)$$

Integrating and rearranging,

$$Y^{\beta} Z^{\alpha} = C \exp(-2\tau) \qquad (14)$$

Using the initial conditions, $C = Y_o^{\beta} Z_o^{\alpha}$, so that Equation (14) supplies a relationship between Y and Z. Using this relationship uncouples the Y and Z equations.

$$\frac{dY}{d\tau} = -Y - \alpha Y^2 + \alpha Z_o Y_o^{\beta/\alpha} Y^{1-\beta/\alpha} \exp(-2\tau/\alpha) \qquad (15)$$

$$\frac{dZ}{d\tau} = \begin{cases} 0 & \beta(Y-Z) \geq 1 \\ -Z - \beta Z^2 + \beta Y_o Z_o^{\alpha/\beta} Z^{1-\alpha/\beta} \exp(-2\tau/\beta) & \beta(Y-z) \leq 1 \end{cases} \qquad (16)$$

Rigorous solutions to these equations have not been attempted because of the extent of the effort required. Numerical methods must be resorted to and/or their properties may be investigated by solutions of simpler, approximate equations.

F. FLAME PHOTOMETRY STUDIES

The flame photometric method for the analysis of phosphorus was of particular interest because of the simplicity of use, ease of sample preparation, high sensitivity, and the possibility of coupling the flame photometer directly to the Technicon for automatic analysis of the test solutions. A preliminary literature search indicated that the flame emission from phosphorus compounds should not be a function of molecular structure (Ref. 7). A preliminary experimental program was carried out to examine the feasibility of the method.

The spectra of flames containing eight different organophosphorus compounds were investigated with a Hilger Watts quartz prism spectrograph (Ref. 7). The band heads were the same as those given by Pearse and Gaydon (Ref. 8) for PO^* indicating that excited PO was formed by burning all the organophosphorous compounds investigated. One of the strongest bands was in the ultraviolet at 335 nm. The spectra appeared to be structure dependent, but the qualitative nature of the experiment precluded a definitive conclusion at this point. Several experiments utilizing an alcholol burner containing tributyl butyl phosphonate with a monochromator-photomultiplier arrangement indicated that the relative intensity at 335 nm was proportional to the concentration.

This UV approach for the analysis of phosphorus was discontinued on the basis of the work of Brody and Chaney which indicated that the HPO visible emission (526 nm) led to higher sensitivity (Ref. 9).

The simple wick type alcohol burner was not useful for quantitative studies at low concentrations so a commercial Jarrel Ash burner was purchased. The Jarrel-Ash "Hetco" burner is an external mix total consumption burner designed on intraconal gas flow principle. The velocity of the oxidizing gas (air) passing the capillary orifice produces a vacuum in the capillary. The vacuum is used to draw a sample up the capillary aspirator and into the sheer stream of oxidizing agent. The detector consists of a multiplier phototube (S11 response) and an interference filter with a peak transmission at 5260Å (110Å bandwidth at half maximum). A potential of 950 volts was applied to the PM and the signal was amplified with a Hewlett Packard Model 425 microvolt meter.

The purpose of this investigation was to determine the lower limit of detection of phosphorus in organophosphorous compounds. Methanol and isopropanol were used as solvents because of their low background emission at 5260Å. When the flow rates of hydrogen and air were adjusted to give the maximum signal in either solvent, the calibration curves were identical. The lower limit of detection of phosphorus (50 ppm solvent) (Figure 11) was decreased to 0.5 ppm by bucking out the solvent emission and increasing the aspiration rate of the solvent. This is considerably better than the results which can be obtained with emission spectroscopy (50-100 ppm) and comparable to conventional flame photometry results of 1 ppm of phosphorus (inorganic).

The lower limit of detection might be increased further by using a concave mirror behind the flame with its center of curvature in the flame and by placing a lens system between the filter and the PM tube to increase the collection efficiency.

The emission spectrum of BiS in a hydrogen rich flame was taken with a Perkin-Elmer Model 99G scanning spectrometer (0.5 mm slits). The detector was an EMI 9558Q photomultiplier. The spectrum (Figure 12) uncorrected for spectrometer response, shows that the band spectra of BiS is not well resolved. This may be attributed to the presence of the solvent and the noise problem.

This visible flame photometric method for phosphorus does not appear to be satisfactory for total phosphorus analysis because the 526 nm emission is a function of molecular structure. This was first noticed after the UV spectra taken with the Hilger Watts Spectrograph were carefully analyzed. At similar phosphorus concentrations and approximately

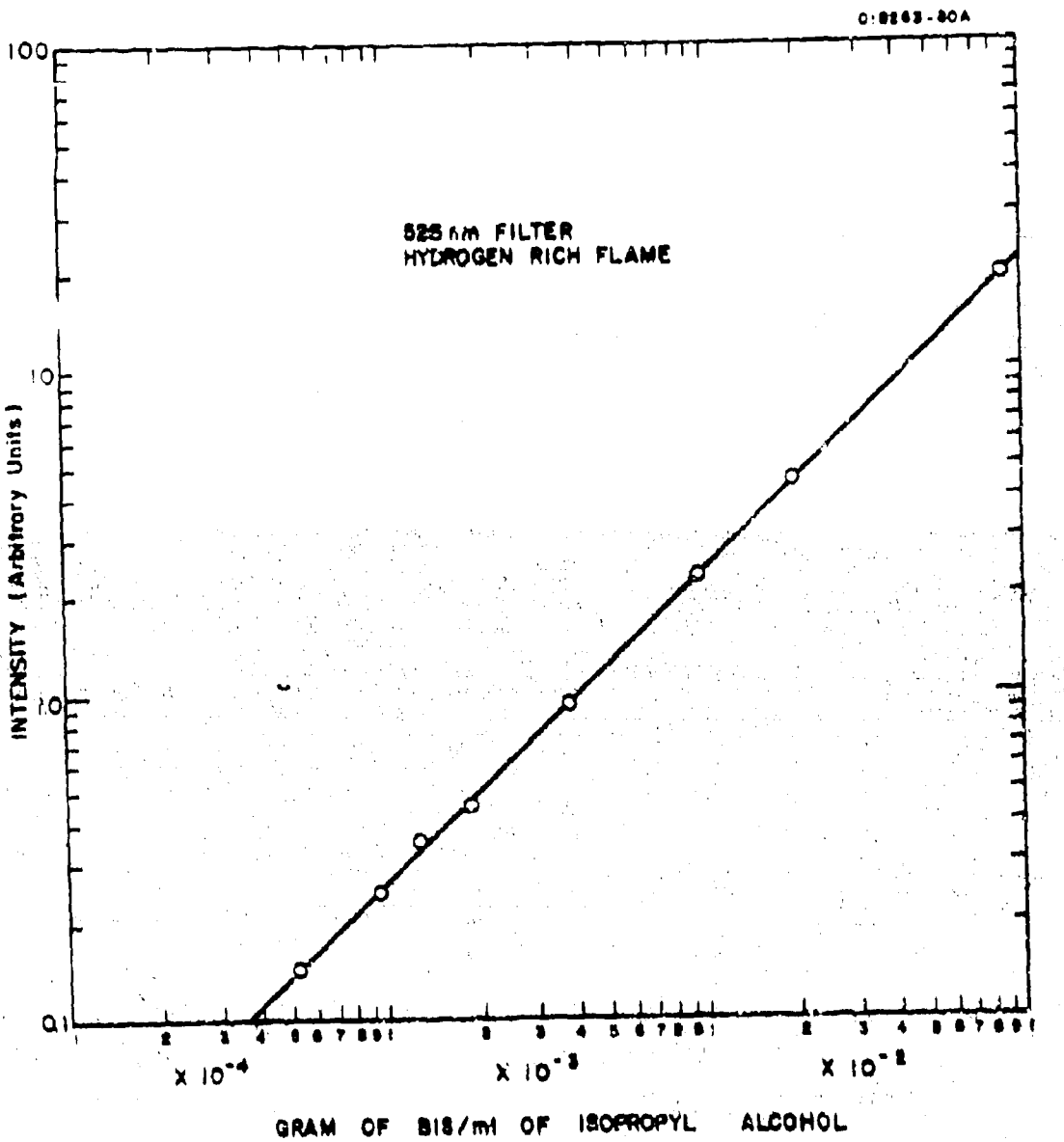

Figure 11. Calibration curve for Bis using flame photometric detector.

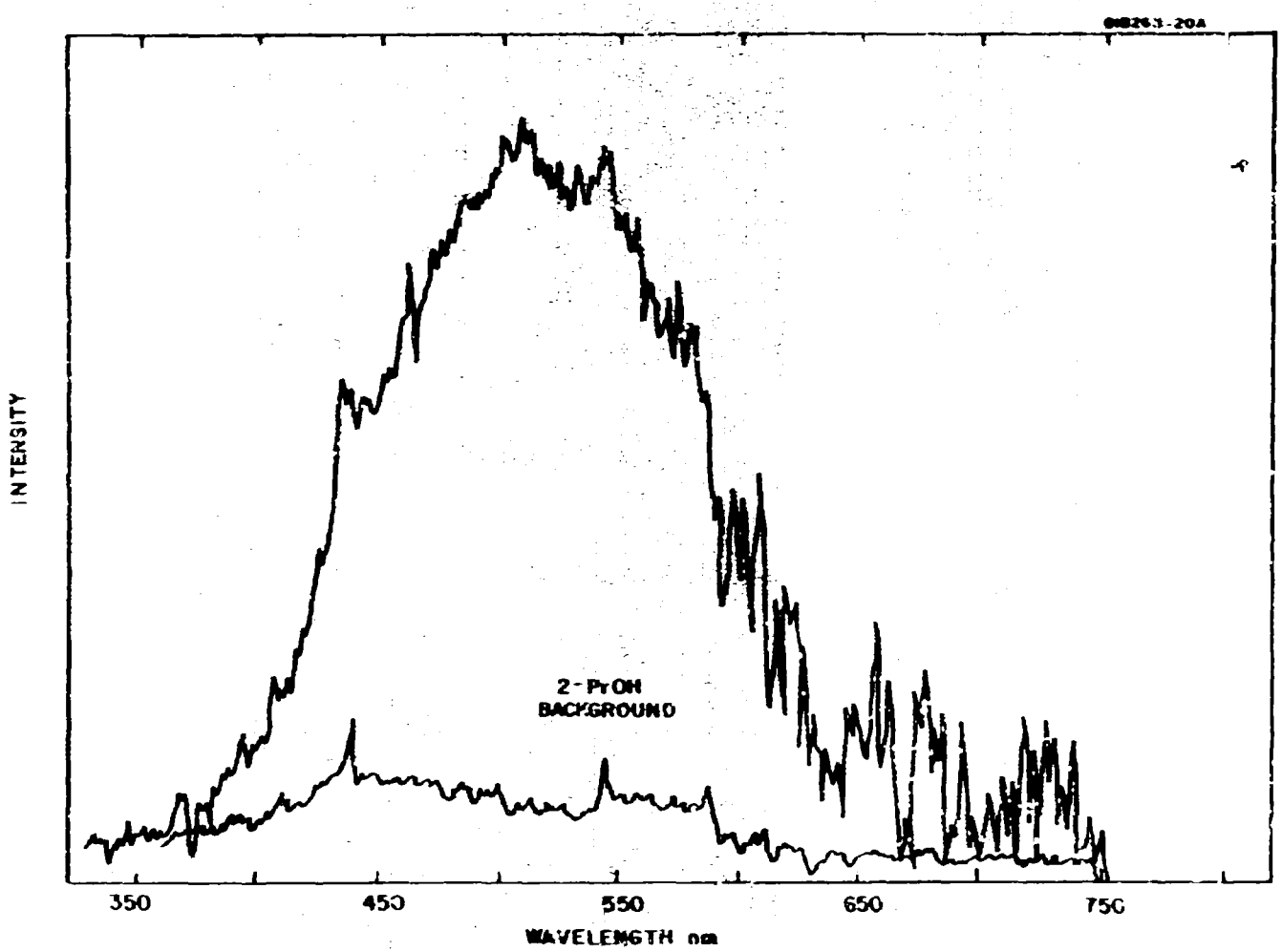

Figure 12. Flame spectrum of Bis in isopropyl alcohol.

the same conditions, the darkening of the film varied with different organophosphorous compounds. Although these data are only qualitative, they indicate that the amount of PO produced is influenced by structure. Brody and Chaney found a variation of emission at 526 nm for two pesticides of different structure. At 526 nm the emission is due to the following process (Ref. 10).

$$H + PO + M \longrightarrow HPO^{*} + M$$

$$HPO^{*} \longrightarrow HPO + h\nu$$

Since the amount of PO formed varies with structure, the emission in a hydrogen rich flame at 526 nm would also vary. This method, although very sensitive and convenient will not be accepted for the assessment system because of the dependence on structure.

G. MASS DECAY INVERSION ANALYSIS

The approaches that have been used to deduce the initial particle size distribution from measurement of mass decay (gravitational settling) in a stirred chamber can generally be grouped into two classes.

The first class is an empirical approach and is characterized by the fact that the form of the particle size distribution is assumed a priori and then tested for goodness of fit to the observed mass decay numerical methods using a suitable minimization criterion. This type of solution provides a quantitative estimate of the gross particle statistics plus a qualitative picture of the initial mass distribution which characterizes the observed decay measurements.

The empirical approach lacks the property of uniqueness; i.e., several distributions may give approximately equal good fits to the observed data. Hence, the conclusion cannot be drawn from these results that the assumed distribution which yields the best fit is the general solution. Experience has shown, however, that assumed mass distributions which fit equally well, in general, will exhibit similar gross features in the solution even though derived from differing mathematical forms. Thus, the empirical approach provides a method for determining these features and the choice of the assumed distribution becomes a matter of convenience.

A second approach to the analysis of mass decay data does not involve an assumption on the form of the initial particle distribution but attempts to derive it directly by solution of the integral equation describing the mass decay process. The solution is developed numerically by utilizing an appropriate quadrature formula to obtain a set of

simultaneous linear equations which then may be solved by standard matrix inversion techniques. The difficulty with this approach is that the matrix to be inverted is generally near singular, and even small errors in the data will produce unreliable results. To overcome this difficulty, two modifications to the basic approach have been attempted; one is to apply a smoothing operator to reduce the effect of errors and the other is to develop a nonlinear solution. Both of these techniques will be discussed in greater detail in the following sections.

1. Empirical Analysis

The loss of material as a function of time in a chamber due to gravitational precipitation under conditions of continuous stirring can be expressed as

$$\frac{M(\tau)}{M(0)} = \int_a^b \exp\left[-Cd^2\tau\right] f(d)\, \delta d \qquad (17)$$

where

$M(\tau)$	=	mass concentration at time τ
$M(0)$	=	mass concentration at time $\tau = 0$
d	=	particle diameter
$f(d)$	=	mass distribution function
$\exp\left[-Cd^2\tau\right]$	=	decay function for Stokes' settling
C	=	a constant

and a and b define a range of expected diameters. It remains to specify the form of f(d) and to adjust the parameters of the assumed distribution to fit the experimental data.

Previous studies have assumed that f(d) can be represented by the log-normal distribution. The work conducted on empirical methods during the current reporting period consisted of testing several other distribution functions and comparing these with the solutions obtained for the log-normal.

One of the functions tested is the Rayleigh (Ref. 19) probability distribution. This distribution is a special case of the bivariate normal distribution and is frequently employed in radio communications engineering. The distribution is unimodal and positively skewed; a single parameter characterizes the curve. The principal advantage of this function to the current application is that its form permits direct integration of Equation (17). The single parameter then can be estimated from the observed data points.

A second model tested was based on the gamma probability distribution function. This is a two-parameter distribution which is unimodal and can assume both symmetric and skew forms depending on the value of the parameters. The exponential function is a special case of the gamma distribution. Using the gamma distribution in Equation (17) does not permit direct integration, necessitating a trial and error method for estimating the best fit parameter values.

Tests conducted with these models as well as those with the log-normal distribution indicated that approximations to a solution could be derived but that these generally satisfied one segment of the observed data better than another. This is a consequence of the characteristic of the test data which indicates a rapid depletion of large particles from the aerosol cloud during the initial period after dissemination followed by a residual decay of the smaller particles. Unimodal models for the initial mass distribution including those discussed above do not possess sufficient flexibility to satisfy both of these features simultaneously. As a result, further research with empirical methods was directed at developing bimodal mass distributions.

The use of bimodal distributions for studying coagulating aerosols has been reported earlier by Dalla Valle, Orr and Blocker (Ref. 7). The analytic form of this model was not convenient for the current application and a simpler function was desired. For this purpose, a three-parameter bimodal model was synthesized from the sum of two Rayleigh distributions. This sum can be expressed as

$$f(d) = K \frac{d}{\omega_1^2} \exp\left[-d^2/2\omega_1^2\right] + (1-K) \frac{d}{\omega_2^2} \exp\left[-d^2/2\omega_2^2\right] \quad (18)$$

where ω_1 and ω_2 are parameters of the distributions, K and (1-K) are the fractional mix of each. Hence, there are three parameters to be specified namely ω_1, ω_2 and K. Substituting in Equation (17) for f(d) and integrating, results in

$$\frac{M(\tau)}{M(0)} = \left[- \frac{K \exp\left[-d^2 \left(\omega_1^2 C\tau + 1\right)/2\omega_1^2\right]}{2\omega_1^2 C\tau + 1} - \frac{(1-K) \exp\left[-d^2 \left(2\omega_1^2 C\tau + 1\right)/2\omega_2^2\right]}{2\omega_2^2 C\tau + 1} \right]_{d_1}^{d_2} \quad (19)$$

Assuming that d_2 is sufficiently large so that the value of this function is negligibly small at the upper limit and that d_1 is sufficiently small

so that the exponential terms approach unity at the lower limit, the final result becomes

$$\frac{M(\tau)}{M(0)} = \frac{K}{2\omega_1^2 C\tau + 1} + \frac{(1-K)}{2\omega_2^2 C\tau + 1} \qquad (20)$$

This last assumption may require values of d_1 and/or d_2 which are somewhat outside the Stokes' Law region, but the resultant error will be neglected for the time being.

This model was tested on the same observed mass decay data previously used to test the unimodal models. Two algorithms were used to estimate the model parameters in Equation (20). One of these is the classical Newton-Raphson method for the solution of nonlinear equations (Ref. 12). For the current application, this technique was constrained to seek values for the model parameters which minimized the root-mean-square (rms) error between the observed data and the model values. Similarly, a more recent iteration technique developed by Marquardt (Ref. 13) was used, subject to the same minimization criterion. Both of these methods were programmed for automatic calculation by the IBM 1620 computer. The availability of both schemes provided an alternative when stable solutions were difficult to obtain. They also provided a means for validating that the given solution represented a global rms minimum and not just a local minimum.

The bimodal model was used, among other things, to compare the results of a test series using both Bis and VX fill with a No. 22 plastic sphere as the disseminator. The results from these inversion analyses for the mass distribution in the initial aerosol cloud have been reported separately* and are summarized in Table 6. The data presented give the distribution parameters for the model, the mass recovery at 24 minutes predicted by the model and the rms error of model fit to the data. The model parameter ω_1 indicates the mode diameter of the small size particles in the initial aerosol cloud while ω_2 gives the mode for the large size components. In several tests these values are given as either an arbitrarily small value ($< 10^{-3}$) or as an arbitrarily large value ($> 10^{3}$). The latter case is used to indicate that the solution was not capable of discriminating from the decay measurements a stirred settling of the large size component but rather this material is depleted from the cloud by other loss processes. In the former case, the arbitrarily small size diameter indicates that the model solution could not detect any sedimentation in the small size component over the time duration of the test. The implication is that a very fine aerosol exists in the chamber as a residual mass.

---

*Letter Report to Mr. Donald Buck, 21 April 1967, also included in this report were selected results from tests employing other fills and/or different dissemination devices.

TABLE 6

SUMMARY OF INVERSION ANALYSIS RESULTS FOR BIS AND VX TEST SERIES.

Test	Fill	Dissemination	ω_1	ω_2	Mix	R_{24}	rms Error
142	VX	22	9.4μ	$10^3\mu$	24/76%	0.140	20%
146	VX	22	$< 10^{-3}\mu$	111.7μ	18/82%	0.188	25%
155	VX	22	11.7μ	$> 10^3\mu$	59/41%	0.275	11%
159	VX	22	18.6μ	$> 10^3\mu$	48/52%	0.120	20%
166	VX	22	$< 10^{-3}\mu$	84.6μ	10/90%	0.113	51%
167	VX	22	9.8μ	180.0μ	50/50%	0.277	11%
168	VX	22	6.0μ	$> 10^3\mu$	43/57%	0.328	7%
169	VX	22	14.3μ	$> 10^3\mu$	42/58%	0.153	11%
170	VX	22	9.6μ	43.6μ	34/66%	0.230	3%
291	VX	22	7.7μ	252.5μ	21/79%	0.14[illegible]	6%
292	VX	22	6.2μ	194.0μ	19/81%	0.47	10%
		Average	10.4μ				
75	BIS	22	4.1μ	164.8μ	53/47%	0.465	15%
86	BIS	22	$< 10^{-3}\mu$	96.1μ	32/68%	0.333	29%
92	BIS	22	$< 10^{-3}\mu$	132.9μ	16/84%	0.167	21%
151	BIS	22	$< 10^{-3}\mu$	52.7μ	43/57%	0.452	15%
152	BIS	22	3.9μ	132.4μ	52/48%	0.461	8%
153	BIS	22	$< 10^{-3}\mu$	$> 10^3\mu$	36/66%	0.335	7%
211	BIS	22	$< 10^{-3}\mu$	57.8μ	11/89%	0.141	24%
		Average	4.0μ			0.336	

A comparison of the performance between these two fills shows (1) that the small size component for VX is larger on the average than that of Bis while (2) the 24-minute recovery for VX is smaller on the average than that for Bis. Both of these effects have been noted in earlier studies; the current model results simply add further evidence to this effect. These results also show a significant improvement in the fit to be observed data and it was concluded that the bimodal model seems to provide a convenient and simple means for analyzing mass decay distributions which are not adequately described in unimodal distributions.

2. Error Analysis

Both the 10^{-3} and 10^{3} solutions discussed above probably arise as a consequence of deficiencies in the data. In the former case, the scatter in the measurements may well mask the slow sedimentation of a relatively small size aerosol cloud. This fact is somewhat evident from the data in Table 6 which shows 10^{-3} solutions generally associated with larger rms errors. In the latter case, the 10^{3} solution reflects the difficulty of obtaining reliable measurements at very short times after the explosive event. The sensitivity of the bimodal model to these measurement problems was investigated by two sets of error analysis calculations.

The first was an error analysis of the inversion model to test its sensitivity to the precision of the mass recovery measurements. The procedure used a simple progressive truncation of a set of mass recovery values from a known particle size distribution. The inversion model was then applied to each set of data and the results compared between the derived distribution and the known distribution. The exact value for the mode of small size fractions in this test was 10 microns, the mode for the large size fractions was 150 microns and the mix between the two-size distributions is in the proportion 35/65 percent. These results are presented below in Table 7. A comparison of the known values with those in Table 7 shows a fair degree of stability even for two-digit accuracy. Also, the results show that the large size fraction seems to be more sensitive to errors in the data than the other two parameters.

TABLE 7

RESULTS FROM INVERSION ANALYSIS OF TRUNCATED DATA.

No. Significant Digits	Mode of Small Size Fraction (ω_1)	Mode of Large Size Fraction (ω_2)	Mixture of Small and Large
1	9.00	129.03	32/68
2	10.35	156.64	36/64
3	10.04	151.69	35/65
4	10.00	150.01	35/65
7	10.00	150.00	35/65

Sensitivity of the solutions to early mass recovery measurements was explored by analyzing approximately a half dozen tests without the assumption of 100 percent recovery at time zero, but with the alternate condition that the mass decay curve satisfy the first measured recovery value. Generally, this first measured point is obtained at 1 minute after detonation. A comparison of the results for these two initial conditions shows reasonable correspondence between the solutions for the small size fraction but major differences in specification of the large particle size distribution. Clearly, most of the large particles fall out or are removed from the cloud within the first minute, with resulting loss of information on their size distribution.

3. Automatic Data Plotting

Toward the latter part of the year, an additional computer program was developed to systematize the presentation of the inversion analysis results. A sample of the preliminary format is shown in the attached Figure 13. The graph shows the observed mass recovery values (crosses) and the computed model mass decay curve (dots). The entire figure was generated by an off-line IBM 870 Document Writing System from program card instructions calculated by the computer. The system requires approximately 7 minutes to plot the graph. Several modifications to this initial format have been suggested and will be added.

4. Direct Inversion by Linear Methods

Techniques for solution of Equation (17) without the aid of a prior assumption on the analytical form of the mass distribution come under the general category of integral equations of the first kind. A brief bibliography of some of the techniques which have been presented in the open literature is given in the references. None of these are entirely satisfactory for analysis of mass decay data and in one form or another are plagued by mathematical problems. One of the most common of these difficulties is the instability introduced into the solutions as a result of noisy data. Numerical experimentation with linear inversion methods on known distributions has shown that something of the order of eight-place accuracy is required in the measurements to recover the initial function. This type of accuracy is rarely available in the measurement of physical systems and certainly not to be expected from mass decay data.

Inversion techniques which deal with problems of instability have been proposed among others by Phillips (Ref. 15) and Twomey (Ref. 16). The basic approach is to express the integral equation as quadratures and apply smoothing constraints to the inversion of the resulting linear system. In the case of Phillips, the smoothing constraint is on minimizing the errors in the second differences of the indicial function. Twomey expands on this general approach by showing how other minimization criteria can be introduced. The general solution is given by the matrix equation

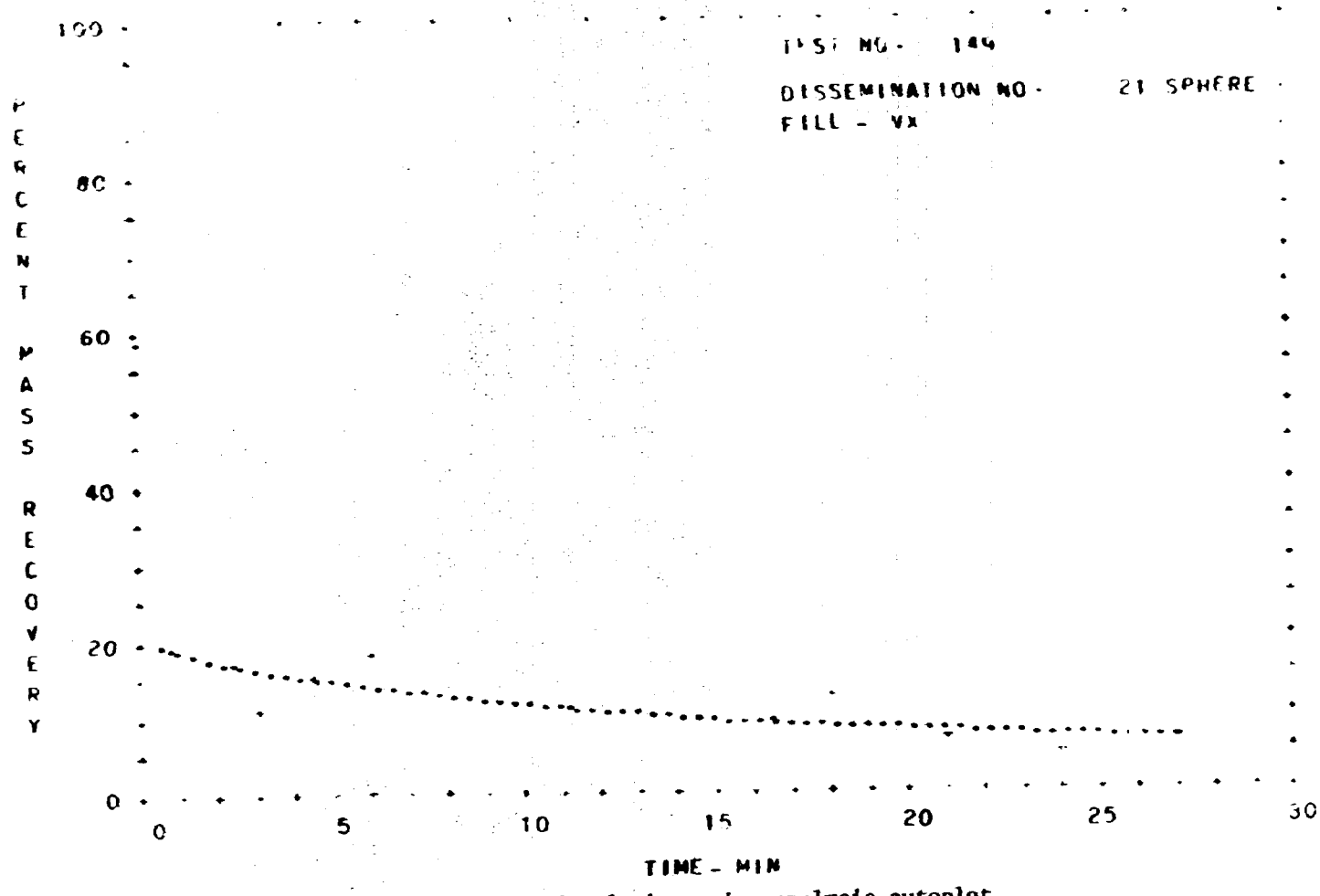

Figure 13. Sample inversion analysis autoplot.

$$f = (A^{*}A + \gamma H)^{-1} (A^{*}M + \gamma p) \qquad (21)$$

where

- f = solution vector
- A = a matrix of quadrature coefficients
- A^{*} = the transpose of A
- γ = the smoothing parameter
- H = a matrix determined by the minimization criterion selected
- M = the observed measurements
- p = a trial solution if one is available

If $p = 0$ and H is the matrix appropriate to the second difference minimization criterion, this solution is equivalent to that given by Phillips but possesses the advantages that (1) only one matrix inversion is required and (2) the A matrix is not required to be square. The latter of these permits solution of an overdetermined system where the number of observations exceeds the number of unknowns.

The utility of this method was tested by means of a set of synthetic mass decay data. These mass decay data were synthesized by assuming a log-normal distribution for f(d) (mass mean diameter = 7.5μ geometric standard deviation = 2.5) and calculating the mass decay using Equation (17). The inversion then was applied to these calculations in an attempt to recover the original log-normal distribution. The results of this experiment are shown in Figure 14 for various values of γ. Comparison of the inversion values to the true distribution shows that the matrix solution corresponding to $\gamma = 0.1$ has recovered the essential features of the original distribution but exhibits consistently greater ordinate values. For $\gamma = 1.0$ the matrix solution begins to lose the symmetric character of the original distribution. It should be noted that selection of an appropriate value of γ is on a trial and error basis and was facilitated in the current experiment by a priori knowledge of f(d). In the general case, selection of a value for γ becomes a more subjective process.

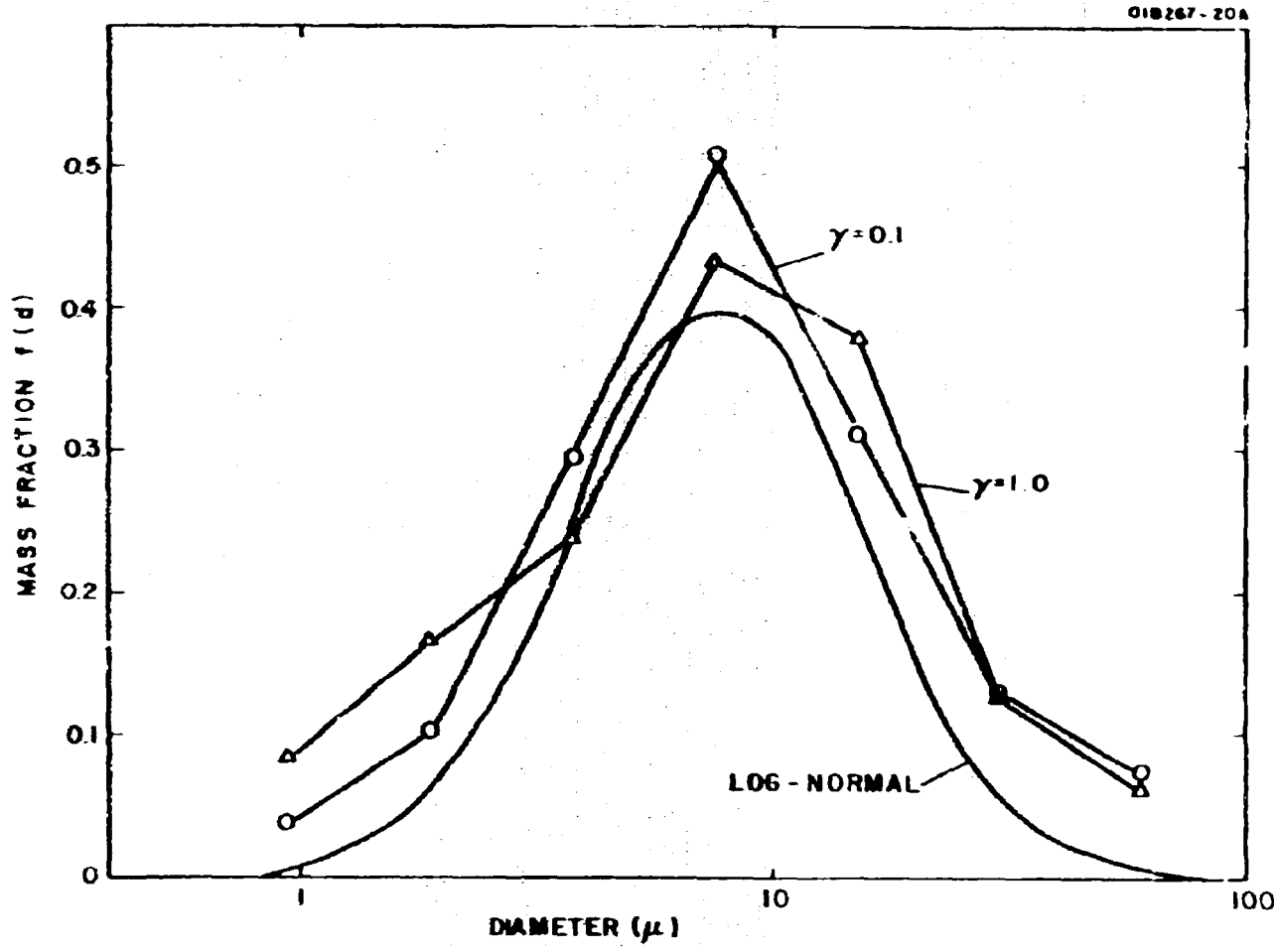

Figure 14. Comparison of assumed log-normal distribution and results of matrix inversion for different levels of smoothing.

5. Nonlinear Inversion Method

The question of how to treat noisy data has most recently been treated in a unique approach by nonlinear methods developed at GCA in another context.* Equation (17) can be expressed as a Laplace transform by making the substitutions

$$u = Cd^2 t_s \text{ and } \lambda = t/t_s \tag{22}$$

in which case we obtain

$$M(\lambda) = \int \exp[-u\lambda]\, g(u)\, du \tag{23}$$

where

$$g(u) = \frac{f(d)}{2Cd\, t_s} \tag{24}$$

In these transformations, t_s is a scale time characteristic for the experiment which can be taken as the time interval between successive measurements. We now assume the function $g(u)$ to be composed of a finite sum of Dirac δ-functions of height ΔP_j at the positions u_j; namely,

$$M(\lambda) = \sum_{j=1}^{n} \Delta P_j X_j^{\ell} \qquad \ell = 0,1,\ldots,2n-1 \tag{25}$$

where

$$X_j = \exp[-u_j]$$

---

*The problem of deriving particle size distributions from observations of mass decay is analogous in many respects to the meteorological problem of inferring the vertical atmospheric temperature structure from measurements of the upwelling radiance intensity. The similarity arises from the fact that in each case the physical process can be described by an integral equation with an exponential decay function as the kernel. The meteorological problem has received considerable attention due to the planned availability of radiance measurements from satellite sensor systems. King (Ref. 16) recently has discussed a nonlinear inversion technique which addresses itself to the two-fold problem of uniqueness and stability of the solution in the presence of noisy data. The above section describes the application of this nonlinear method to the mass decay problem.

The approximation corresponds physically to the assumption that the initial cloud is composed of a series of monodisperse aerosols which are mixed in given proportions. This system of nonlinear equations arises in the construction of Gaussian quadrature formulae and is discussed in texts on applied analysis (Ref. 17). The set can be solved uniquely for the n weights P_i and the n roots X_i by means of the Prony algorithm as described, for example, by Chandrasekhar (Ref. 18).

Since only positive real roots in the $0 < X_i < 1$ permit physical interpretation, all other roots must be rejected and attributed to arising from noise in the data. In most applications of this technique, the weight assigned to these roots is small and their exclusion can be done with reasonable safety. The number of roots which are retained is a qualitative index of the accuracy of the observations.

In a limited number of cases, this nonlinear technique was used to analyze the test data. The limitation on use of this method arises from the requirement that the measurements must be spaced at equal time increments. Relatively few tests satisfied this criterion for sufficient segment of the experiment to warrant use of the technique.

IV. PROGRAM FOR NEXT QUARTER

The general composition of the assessment system is now firm and laboratory programs are to be limited to modest efforts to:

(a) Further development and evaluation of the beta absorption-impactor sampler.

(b) Modifications of the Royco light scattering particle counter for its use in the assessment program.

(c) Further investigations on problems of particle charging with respect to the mass decay of contained aerosols.

The major effort is to be one of system construction and application in the following areas:

(a) Construction of an automated sequential filter sampling system with provisions for variable sampling programming.

(b) Development of a data format competible with computer evaluation of the mass decay curve obtained from sequential filter samples. This activity will be aimed at minimizing errors generated by human intervention in the various steps required to prepare the raw experimental data for its processing by the computer.

LITERATURE CITED

1. Dennis, R., Euling, R., Gussman, R.A., and Hommel, C.O., "Aerosol Dissemination Assessment," First Quarterly Progress Report, U.S. Army Edgewood Arsenal, Contract DA-18-035-AMC-376(A), GCA Technical Report No. 66-22-G (December 1965).

2. Dennis, R. and Hommel, C.O., "Aerosol Dissemination Assessment," Second Quarterly Progress Report, U.S. Army Edgewood Arsenal, Contract DA-18-035-AMC-376(A), GCA Technical Report No. 66-5-G (May 1966).

3. Dennis, R. and Gordon, D., "Aerosol Dissemination Assessment," Third Quarterly Progress Report, U.S. Army Edgewood Arsenal, Contract DA-18-035-AMC-376(A), GCA Technical Report No. 66-20-G (October 1966).

4. Dennis, R. Doyle, A.W., et al., "Aerosol Dissemination Assessment," First Annual Summary Report, U.S. Army Edgewood Arsenal, Contract DA-18-035-AMC-376(A), GCA Technical Report No. 67-2-G (April 1967).

5. Dennis, R., et al., "Aerosol Dissemination Assessment," Fifth Quarterly Progress Report, U.S. Army Edgewood Arsenal, Contract DA-18-035-AMC-376(A), GCA Technical Report No. 67-11-G (September 1967).

6. Dennis, R., et al., "Aerosol Dissemination Assessment," Sixth Quarterly Progress Report, U.S. Army Edgewood Arsenal, Contract DA-18-035-AMC-376(A) GCA Technical Report No. 67-16-G (In press).

7. Dennis, R., et al., "Aerosol Dissemination Assessment," Seventh Quarterly Progress Report, U.S. Army Edgewood Arsenal, Contract DA-18-035-AMC-376(A), GCA Technical Report No. 67-20-G (In press).

8. Pearse, R.W.B., and Gaydon, A.G., Identification of Molecular Spectra Wiley & Son, New York (1963).

9. Brody, S.S. and Chaney, J.E., J. Gas. Ghrom. 4, 42 (1966).

10. Thanh, Lam and Peyron, M., Jl. Chim. Phys. 60, 1289 (1963).

11. Dalla Valle, J.M., Orr, C., and Blocker, H.G., Ind. Eng. Chem. 43, 1377 (1951).

12. Scarborough, J.B., Numerical Mathematical Analysis, Johns Hopkins Press, Baltimore, Md. (1950) p. 191.

13. Marquardt, D.W., "An Algorithm for Least Squares Estimation of Nonlinear Parameters", J. Soc. Indust. Appl. Math. 11, 2, 431-441 (1963).

14. Phillips, D.L., "A Technique for the Numerical Solution of Certain Integral Equations of the First Kind", JACM, 9, 84-97 (1962).

15. Twomey, S., "On the Numerical Solution of Fredholm Integral Equations of the First Kind by the Inversion of Linear Systems Produced by Quadrature", JACM 10, 97-101 (1963).

16. King, J.I.F., "Inversion by Slabs of Varying Thickness", J. Atmos. Sci. 21, 324-326 (1964).

17. Lanczos, C., Applied Analysis, Prentice-Hall, New York (1956).

18. Chandrasekhar, S., Radiative Transfer, Oxford University (1950).

19. Edmundson, H.P., "The Distribution of Radial Error and Its Statistical Application in War Gaming," Opns. Res. 9, 8-21 (1961).

UNCLASSIFIED
Security Classification

DOCUMENT CONTROL DATA - R & D

Security classification of title, body of abstract and indexing annotation must be entered when the overall report is classified

1. ORIGINATING ACTIVITY (Corporate author)
GCA CORPORATION
GCA TECHNOLOGY DIVISION
Bedford, Massachusetts 01730

2a. REPORT SECURITY CLASSIFICATION
UNCLASSIFIED

2b. GROUP
N/A

3. REPORT TITLE
AEROSOL DISSEMINATION ASSESSMENT

4. DESCRIPTIVE NOTES (Type of report and inclusive dates)
Second Annual Report - February 1967 - April 1967

5. AUTHOR(S) (First name, middle initial, last name)
A.W. Doyle, P. Morgenstern, A.M. Sacco, P. Lilienfeld, C.O. Hommel, J.F. McCoy, T.N. Driscoll

6. REPORT DATE
JANUARY 1968

7a. TOTAL NO. OF PAGES
61

7b. NO. OF REFS
19

8a. CONTRACT OR GRANT NO
DA-18-035-AMC-376(A)

8b. PROJECT NO.
1B522301A081

8c.

8d.

9a. ORIGINATOR'S REPORT NUMBER(S)
FR-2, GCA-TR-67-22-G

9b. OTHER REPORT NO(S) (Any other numbers that may be assigned this report)

10. DISTRIBUTION STATEMENT This document is subject to special export controls and each transmittal to foreign governments or foreign nationals may be made only with prior approval of the CO, Edgewood Arsenal, ATTN: SMUEA-TSTI-T, Edgewood Arsenal, Maryland 21010

11. SUPPLEMENTARY NOTES
Chemical agent dissemination

12. SPONSORING MILITARY ACTIVITY
Edgewood Arsenal Research Laboratories
Edgewood Arsenal, Maryland 21010
(D. Buck, Proj. O., Ext. 6105

13. ABSTRACT

The program objectives are to develop, to design, and to fabricate a complete system for the assessment of aerosols dispersed in test chambers. The main activities reviewed are aerosol mass-decay analysis, chamber mixing and material-balance studies, electrostatic effects on chamber aerosols and their evaluation, bioeffectiveness of aerosols, sampling and subsequent data reduction methods required for the determination of aerosol parameters through the mass-decay procedure. The design of an automated sequential filter sampling system is described, as well as initial phases in the development of a beta absorption-impactor instrument. Experiments in the above area were conducted both in a large(213 m^3) test chamber with explosive dissemination of agent and simulant materials, and in small laboratory chambers with pneumatic aerosol injection.

14. KEYWORDS

Filters
Aerosol
Mass decay
Phosphorus
B-Absorption
Electrostatics
Material balance
Flame photometry
Mass evaluation
Inversion analysis
Perchloric acid oxidation
Automated sequential filter sampling

DD FORM 1 NOV 65 1473 REPLACES DD FORM 1473, 1 JAN 64, WHICH IS OBSOLETE FOR ARMY USE.

UNCLASSIFIED
Security Classification